National Aeronautics and Space Administration

Current and Planned MODIS Land Surface Temperature and Emissivity (LST&E) Products

Glynn Hulley, Simon Hook

Jet Propulsion Laboratory, California Institute of Technology, Pasadena, CA

Special thank to the MODAPS team: Ginny Kalb, Teng-Kui Lim Robert Wolfe, Kurt Hoffman, Jerry Shiles, Sadashiva Devadiga

MODIS Science Team Meeting, Silver Spring, MD, 15-18 April, 2013

Outline

1. Earth science use of LST&E products
2. Theoretical basis
3. Current products and upgrades for C6
4. The MOD21 LST&E product and potential uses
5. Validation of the current products and MOD21
6. Long-term calibration and trends
7. Uncertainty analysis
8. Future Work

Earth Science Use of LST&E

Evapotranspiration (drought monitoring)

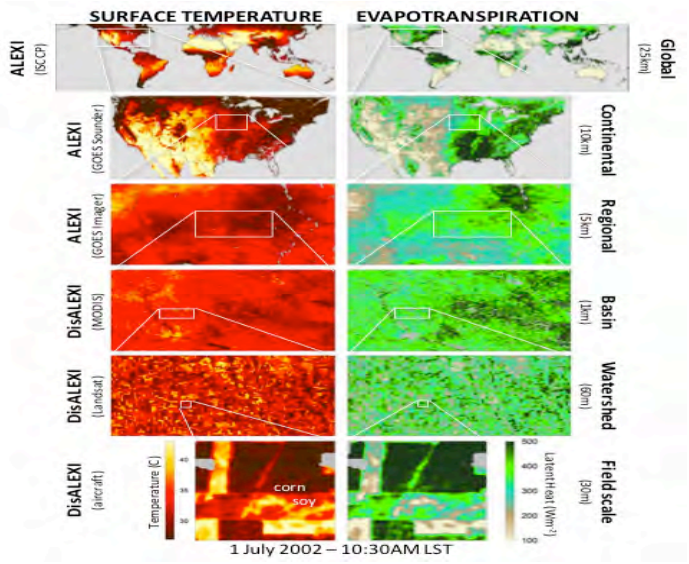

Understanding Climate Change

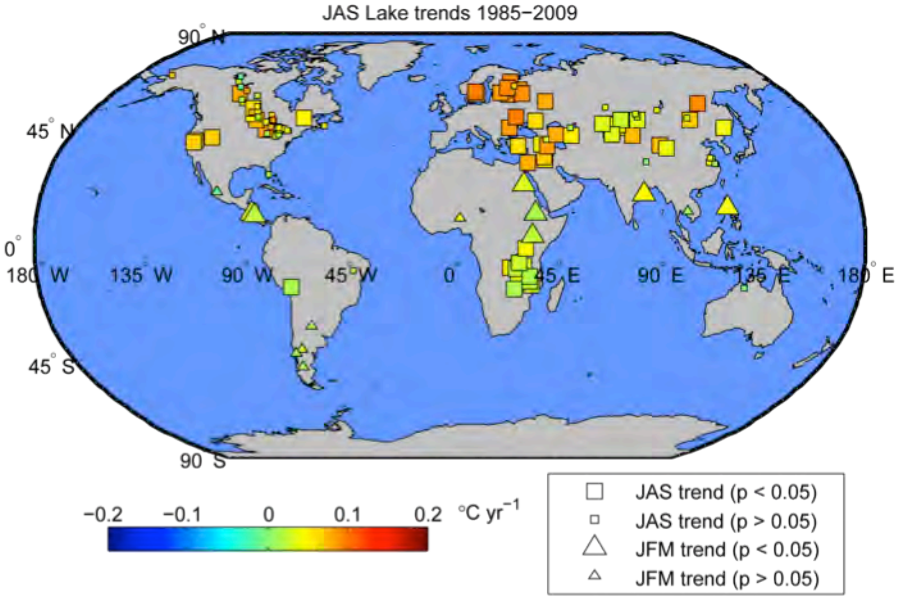

Surface Energy Balance Models

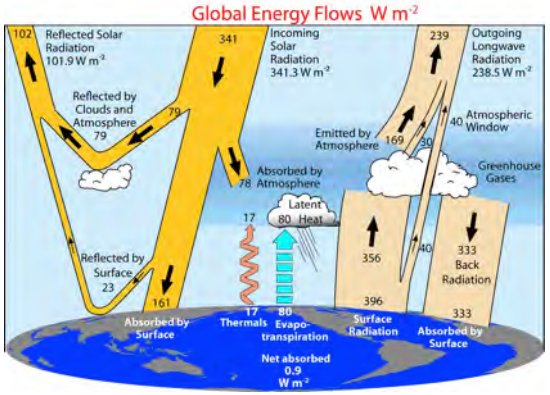

Urban Heat Island Studies

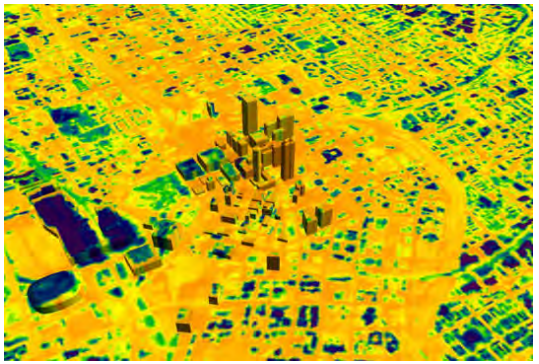

Atmospheric profile retrievals

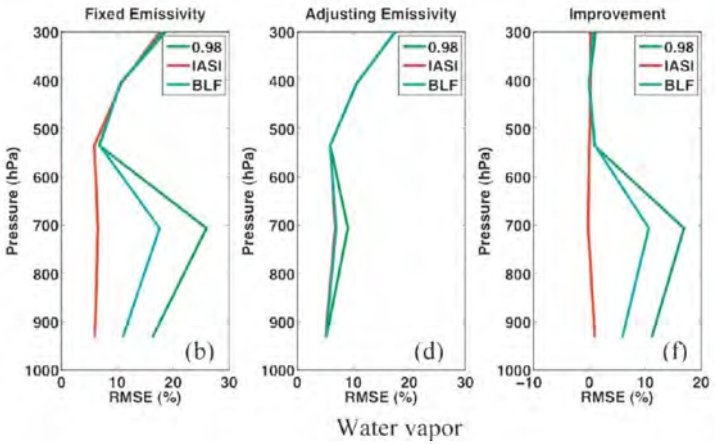

Theoretical Basis: Planck Formula

$$B_\lambda = \frac{C_1}{\lambda^5 \left[\exp\left(\frac{C_2}{\lambda T} \right) - 1 \right]}$$

where :

B_λ = blackbody spectral exitance.

λ = wavelength

T = absolute temperature.

C_1 = first radiation constant.

C_2 = second radiation constant.

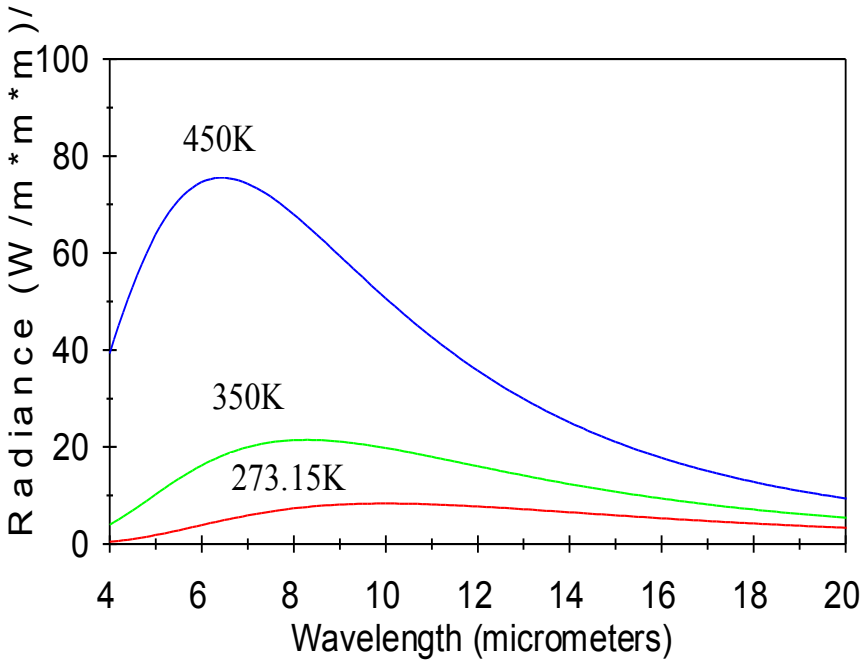

As the temperature increases the peak in the Planck function shifts to shorter and shorter wavelengths

Spectral Emissivity

Materials are not perfect blackbodies, but instead emit radiation in accordance with their own characteristics. The ability of a material to emit radiation can be expressed as the ratio of the spectral radiance of a material to that of a blackbody at the same temperature. This ratio is termed the spectral emissivity:

$$\varepsilon_\lambda = L_\lambda(\text{Material}) / L_\lambda(\text{Blackbody})$$

for a material at a given wavelength, the radiance is:

$$L = \varepsilon\ B\,(\mathrm{T})$$

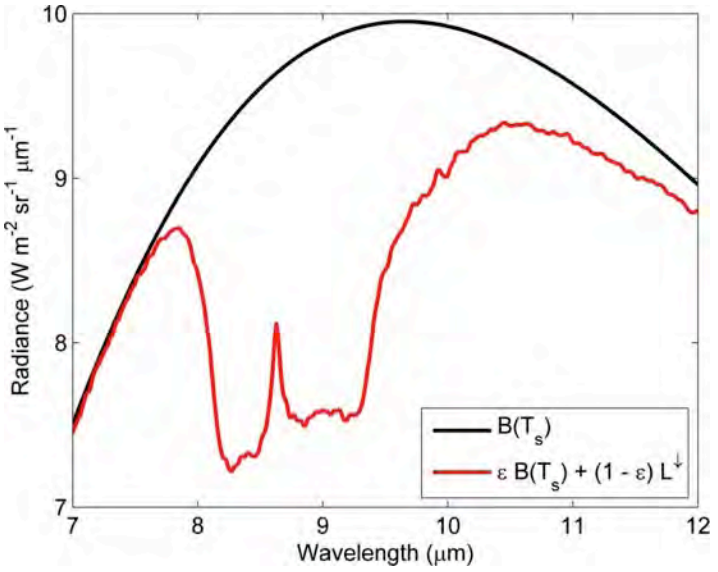

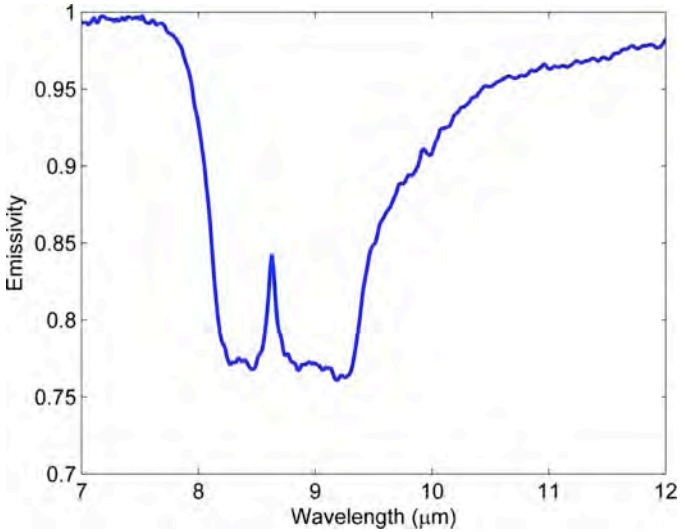

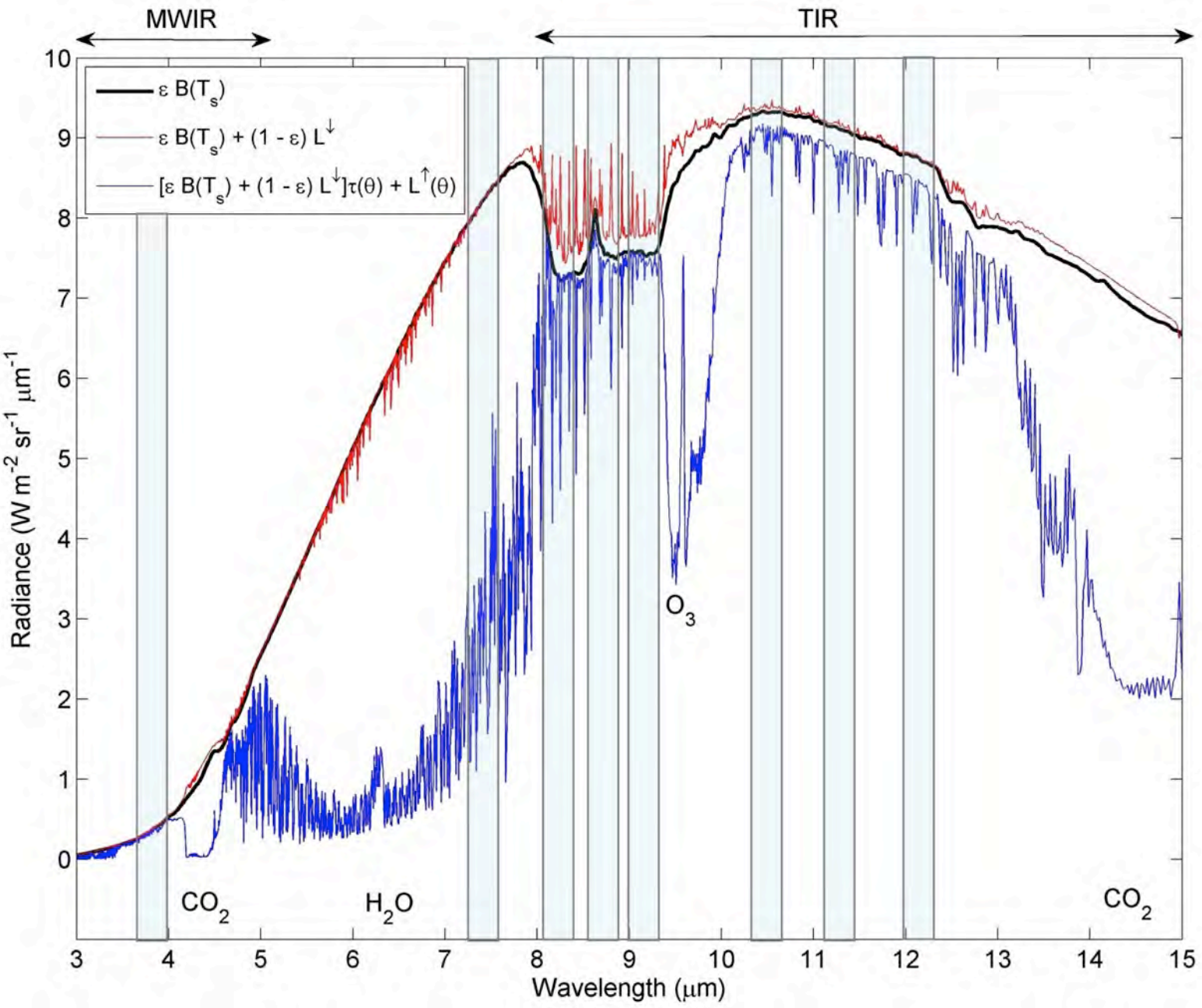
MWIR
TIR
ε B(T_s)
ε B(T_s) + (1 - ε) L↓
[ε B(T_s) + (1 - ε) L↓]τ(θ) + L↑(θ)
Radiance (W m-2 sr-1 μm-1
Wavelength (μm)
CO2
H2O
O3
CO2
0
1
2
3
4
5
6
7
8
9
10
3
4
5
6
7
8
9
10
11
12
13
14
15

Current and planned MODIS LST&E Products

MODIS LST Products	Product Level	Dimensions	Spatial Resolution	Temporal Resolution	Algorithm	Output Products
MOD11_L2	L2	2030 lines 1354 pixels/line	1km at nadir	Swath 2x daily	Split-Window	- LST - Emissivity (bands 31, 32)
MOD11B1	L3	200 rows 200 columns	~5 km (v4) ~6 km (v5)	Sinusoidal 2x daily	Day/Night	- LST - Emissivity (bands 20-23, 29, 31,32)
MOD11C3	L3	360ºx180º Global	0.05º x 0.05º	Monthly	Day/Night + Split-Window	- LST - Emissivity (bands 20-23, 29, 31-32)

None of the current algorithms produce emissivities at 1km resolution

Lessons learned from the validation of the C5 MODIS LST products

1, For the 42 global test sites in different regions used in the C5 LST validation, the LST errors are well within 1K in all sites but five desert sites where some LSTs may be underestimated by more than 3K.

2, The two fundamental causes for the large LST errors in desert regions are
(A) daytime LSTs are beyond the up limit (Ts-air + 16K) used in algorithm development, and
(B) The 0.015 variation range of emis values in MODIS bands 31 and 32 for soil and sand samples (as shown in the variation range of the reflectance values in the right plot) corresponds to large LST errors.

emissivity = 1 - reflectance

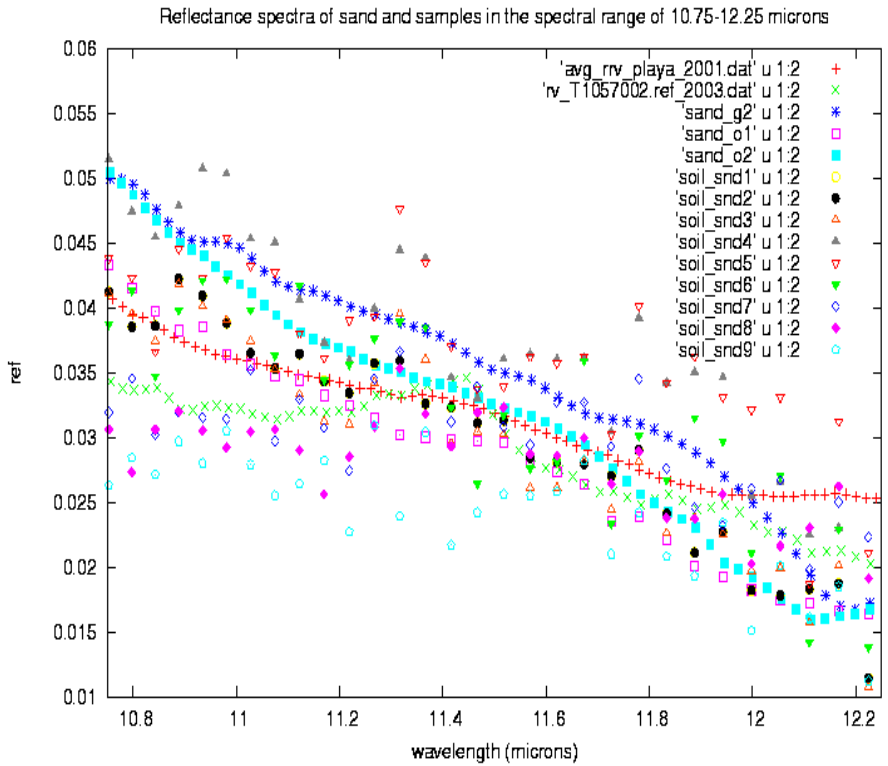

Courtesy Z. Wan

Summary of R-based validation of the C5 MODIS LST products at 32 new sites besides 10 old sites

Site	Location	Latitude, Longitude (°)	Land-cover Type (id #)	MOD11 or MYD11_L2	type of atmos. profiles	mean (std) of LST errors (K)
11	Recife, Brazil	7.96 S, 34.94 W	evergreen forest (2)	MOD11	radiosonde	0.4 (0.4)
12	Moree, Australia	29.555 S, 149.86 E	open shrubland (7)	MOD11	radiosonde	-0.8 (0.9)
13	Port Elizabath, S. Africa	33.95 S, 23.59 E	evergreen forest (2)	MYD11	radiosonde	-0.2 (0.9)
14	WLT Alert,Canada	82.4 N, 62.33 W	shrubland (7)/snow(15)	MOD11	radiosonde	0.2 (0.8)
15	South Pole	89.95 S, 0.05 E	snow/ice (15)	MOD11	radiosonde	-0.5 (0.6)
16	McMurdo,Antarctica	77.75 S, 164.1 E	snow/ice (15)	MOD11	radiosonde	0.1 (0.3)
17	Dye-2, Greenland	66.481 N, 46.28 W	snow/ice (15)	MOD11	NCEP	0.0 (0.5)
18	Summit, Greenland	72.58 N, 38.475 W	snow/ice (15)	MOD11	NCEP	0.1 (0.5)
19	Cherskij, Russia	68.75 N, 161.27 E	snow (15)/shrubland(7)	MOD11	radiosonde	0.3 (0.5)
20	Gaze, Tibet, China	32.3 N, 84.06 E	open shrubland (7)	MOD11	NCEP	-0.6 (0.2)
21	Hainich, Germany	51.079 N, 10.452 E	mixed forest (5)	MOD/MYD	radiosonde	-0.3 (0.5)
22	Paris, France	48.8 N, 2.35 E	urban (13)	MYD11	radiosonde	0.1 (0.4)
23	near Paris, France	48.45 N, 2.25 E	cropland (12)	MYD11	radiosonde	0.0 (0.6)
24	Nimes, France	43.84 N, 4.37 E	urban (13)	MYD11	radiosonde	0.1 (0.4)
25	near Nimes, France	43.828 N, 4.535 E	cropland (12)	MYD11	radiosonde	-0.1 (0.6)
26	Milan, Italy	45.485 N, 9.21 E	urban (13)	MYD11	radiosonde	-0.3 (0.7)
27	near Milan, Italy	45.297 N, 9.26 E	cropland (12)	MYD11	radiosonde	-0.3 (0.6)
28	Cuneo, Italy	44.53 N, 7.62 E	cropland (12)	MYD11	radiosonde	0.0 (0.5)
29	Payerne, Switzerland	46.855 N, 6.965 E	cropland (12)	MYD11	radiosonde	0.0 (0.5)
30	Nenjiang, China	49.07 N, 125.23 E	cropland(12)/snow(15)	MOD11	radiosonde	-0.3 (0.6)
31	Yichun, China	47.76 N, 128.88 E	mixed forest (5)	MOD11	radiosonde	0.1 (0.6)
32	Harbin, China	45.73 N, 126.65 E	urban (13)	MOD11	radiosonde	0.2 (0.8)
33	near Harbin, China	45.9 N, 127.1 E	cropland (12)	MOD11	radiosonde	0.1 (0.8)
34	Algiers, Algeria	36.72 N, 3.03 E	urban (13)	MOD11	radiosonde	-0.2 (0.9)
35	Dar-El-Beida,Algeria	36.65 N, 3.28 E	cropland (12)	MOD11	radiosonde	-0.5 (0.7)
36	Niamey, Niger	13.5 N, 2.14 E	urban (13)	MOD11	radiosonde	-0.3 (1.0)
37	Near Niamey, Niger	13.58 N, 2.07 E	grassland (10)	MOD11	radiosonde	-0.9 (1.1)
38	Tamanrasset, Algeria	22.856 N, 5.455 E	bare soil (16) in desert	MOD/MYD	radiosonde	-1.9 (1.2)
39	Bechar, Algeria	31.62 N, 2.33 W	bare soil (16) in desert	MOD/MYD	radiosonde	-1.5 (0.6)
40	Farafra, Egypt	27.04 N, 27.97 E	bare soil (16) in desert	MYD11	radiosonde	0.9 (0.4)
41	SVU, Egypt	26.285 N, 32.78 E	bare soil (16) in desert	MYD11	radiosonde	-1.6 (0.5)
42	In-salah, Algeria	27.18 N, 2.6 E	bare soil (16) in desert	MOD/MYD	radiosonde	-3.0 (0.8)

Courtesy Z. Wan

New Refinements for the C6 Daily MODIS LST PGE (PGE16)

Two new sets of coefficients in the generalized split-window algorithm were developed for bare soil/sand pixels in separate conditions of daytime and nighttime, and the range of (LST – Ts-air) is set as from 8 – 29K for daytime LST and from -10 – 4K for nighttime LST, in order to well address the problems of very wide temporal variation range for daytime LST changes and possible large uncertainties in Ts-air values provided by the M*D07_L2 products.

Table 1A, Mean and standard deviation of LST difference values in the C6, C5 and C41 MOD11B1 Products at some typical sites in 2007.

site name	latitude/longitude	land cover type	daytime LST		nighttime LST	
			C5 - C6	C41 – C6	C5 – C6	C41 – C6
Lake Tahoe	39.11, -120.03	inland lake	0.01 ±0.16	0.43 ±0.16	-0.06 ±0.18	-0.12 ±0.18
Mojave	35.129, -115.65	open shrublands	0.01 ±0.17	1.48 ±0.19	-0.12 ±0.17	1.41 ±0.17
Tamanrasset	22.78, 5.52	bare soil/sand	-2.84 ±0.16	-0.68 ±0.20	-1.80 ±0.17	-0.44 ±0.19
In-salah	27.22, 2.5	bare soil/sand	-3.50 ±0.20	-0.20 ±0.24	-2.27 ±0.17	-0.01 ±0.18
Sonoran	31.9, -114.47	bare soil/sand	-3.27 ±0.18	-1.01 ±0.22	-2.71 ±0.18	-1.18 ±0.31
north Tassili	27.0, 7.65	bare soil/sand	-3.79 ±0.19	-0.70 ±0.24	-2.95 ±0.16	-0.48 ±0.17

Table 2A, Mean and standard deviation of emissivity values in band 29 in the C6, C5 and C41 MOD11B1 Products at some typical sites in 2007.

site name	latitude/longitude	land cover type	mean and standard deviation in the whole year		
			C6	C5	C41
Lake Tahoe	39.11, -120.03	inland lake	0.986 ± 0.007	0.985 ± 0.007	0.982 ± 0.011
Mojave	35.129, -115.65	open shrublands	0.915 ± 0.020	0.921 ± 0.020	0.923 ± 0.016
Tamanrasset	22.78, 5.52	bare soil/sand	0.926 ± 0.009	0.917 ± 0.018	0.931 ± 0.020
In-salah	27.22, 2.5	bare soil/sand	0.820 ± 0.018	0.856 ± 0.062	0.806 ± 0.038
Sonoran	31.9, -114.47	bare soil/sand	0.763 ± 0.022	0.838 ± 0.075	0.759 ± 0.032
north Tassili	27.0, 7.65	bare soil/sand	0.716 ± 0.019	0.814 ± 0.097	0.714 ± 0.029

Courtesy Z. Wan

Split Window: Classification versus actual emissivity

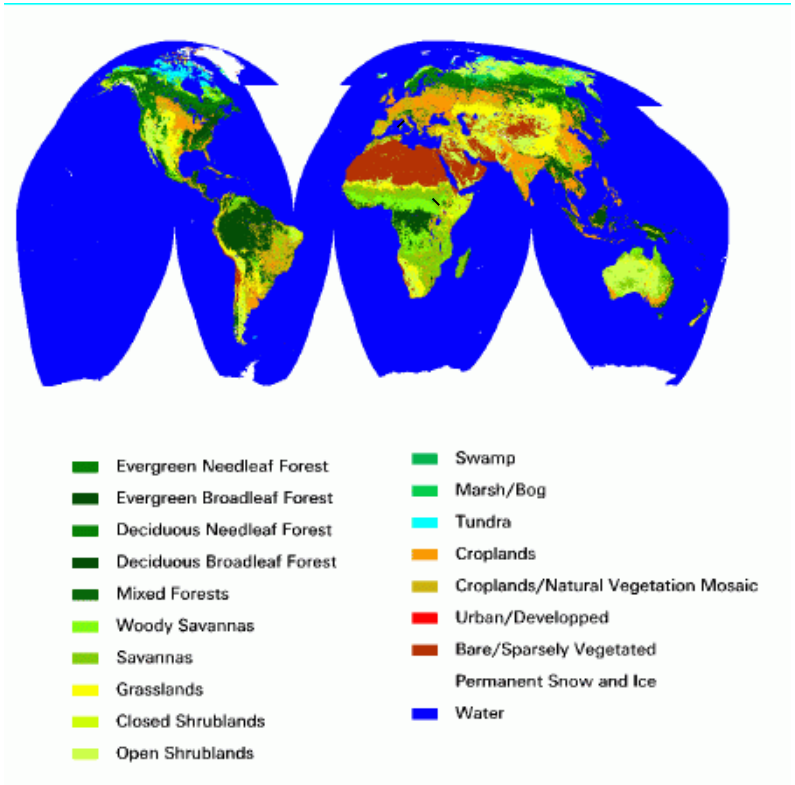

MOD11 band 32

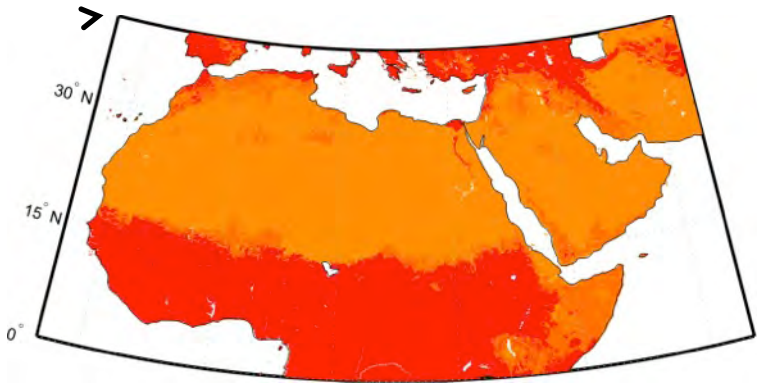

MOD21 band 32

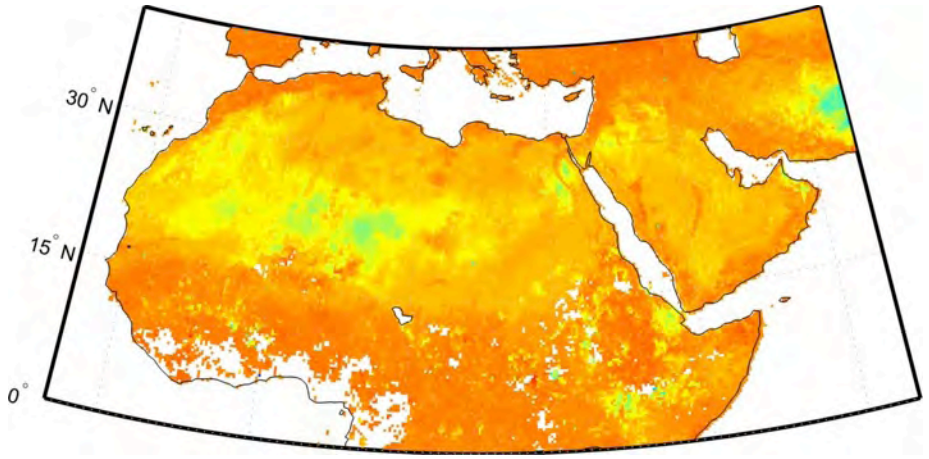

MOD 11 classified as bare and assigned single emissivity but a wide range in emissivity as seen with MOD21

Current and planned MODIS LST&E Products

MODIS LST Products	Product Level	Dimensions	Spatial Resolution	Temporal Resolution	Algorithm	Output Products
MOD11_L2	L2	2030 lines 1354 pixels/line	1km at nadir	Swath 2x daily	Split-Window	- LST - Emissivity (bands 31, 32)
MOD11B1	L3	200 rows 200 columns	~5 km (v4) ~6 km (v5)	Sinusoidal 2x daily	Day/Night	- LST - Emissivity (bands 20-23, 29, 31,32)
MOD11C3	L3	360ºx180º Global	0.05º x 0.05º	Monthly	Day/Night + Split-Window	- LST - Emissivity (bands 20-23, 29, 31-32)
MOD21_L2	L2	2030 lines 1354 pixels/line	1km at nadir	Swath 2x daily Monthly	ASTER-TES	- LST - Emissivity (bands 29, 31, 32)

** Planned, dynamic emissivity retrieval algorithm same as used with ASTER. Produces T&E at 1km resolution

The Temperature Emissivity Separation (TES) Algorithm (MOD21)

Surface Radiance:

Observed Radiance

$$L_{surf,i} = e_i \cdot B_i(T_S) + (1 - e_i) \cdot \overline{L}_i^{\downarrow} = \frac{L_i(\theta) - L_i^{\uparrow}(\theta)}{\tau_i(\theta)}$$

- **Atmospheric Parameters:** $\tau_i(\theta)$, $L_i^{\uparrow}(\theta)$, $L_i^{\downarrow}(\theta)$

  Estimated using radiative transfer code such as MODTRAN with Atmospheric profiles and elevation data

Calibration curve for MODIS bands 29, 31, 32:

$$\varepsilon_{\min} = 0.994 - 0.687 \cdot MMD^{0.737}$$

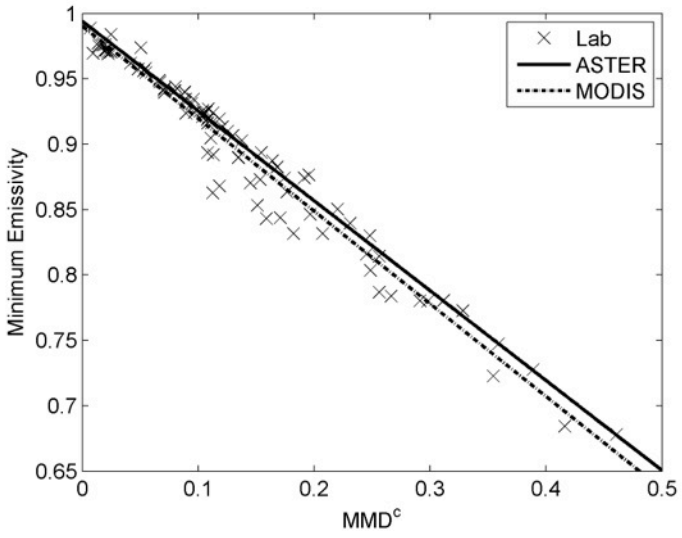

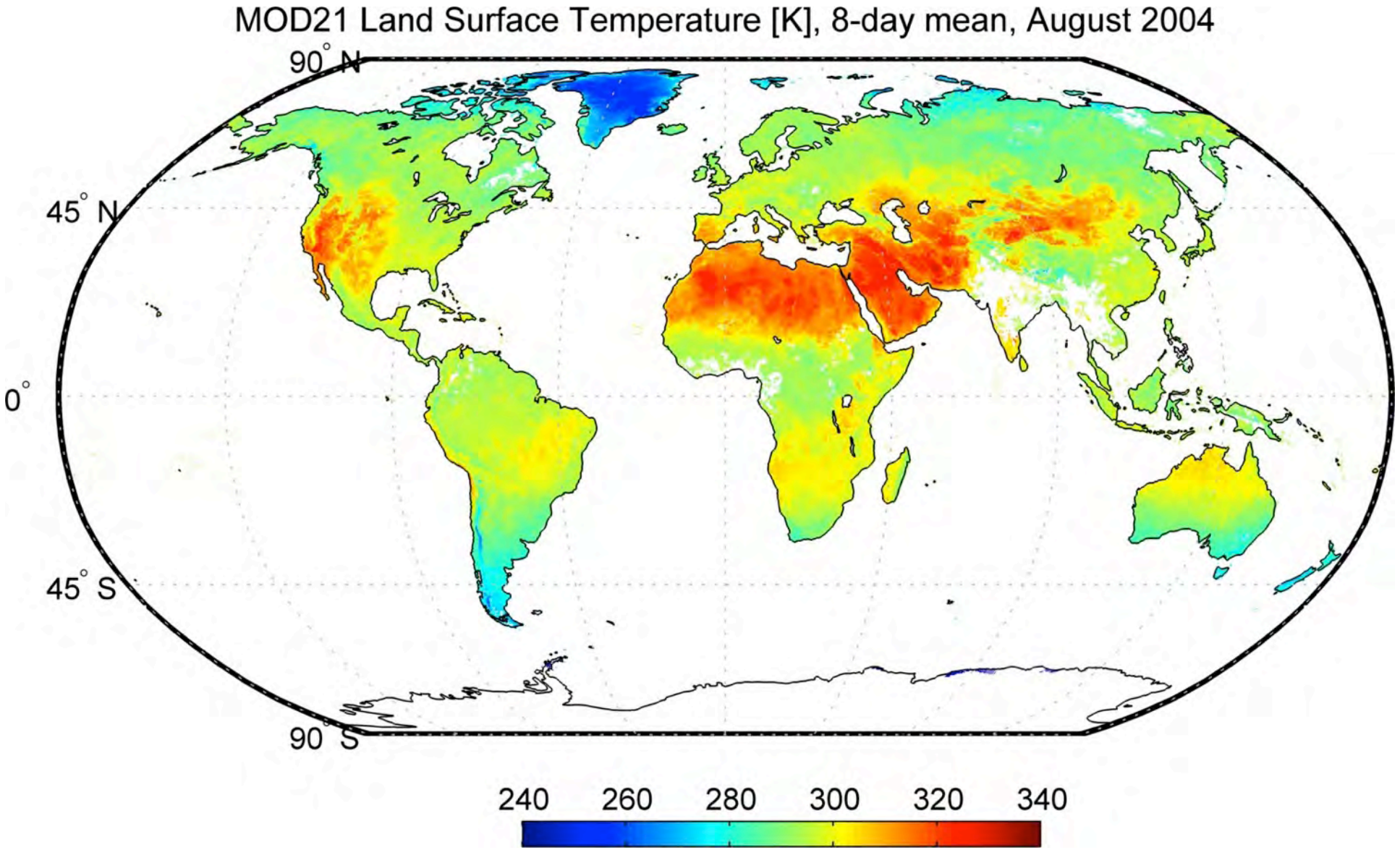

Generated using prototype MOD21 algorithm at MODAPS

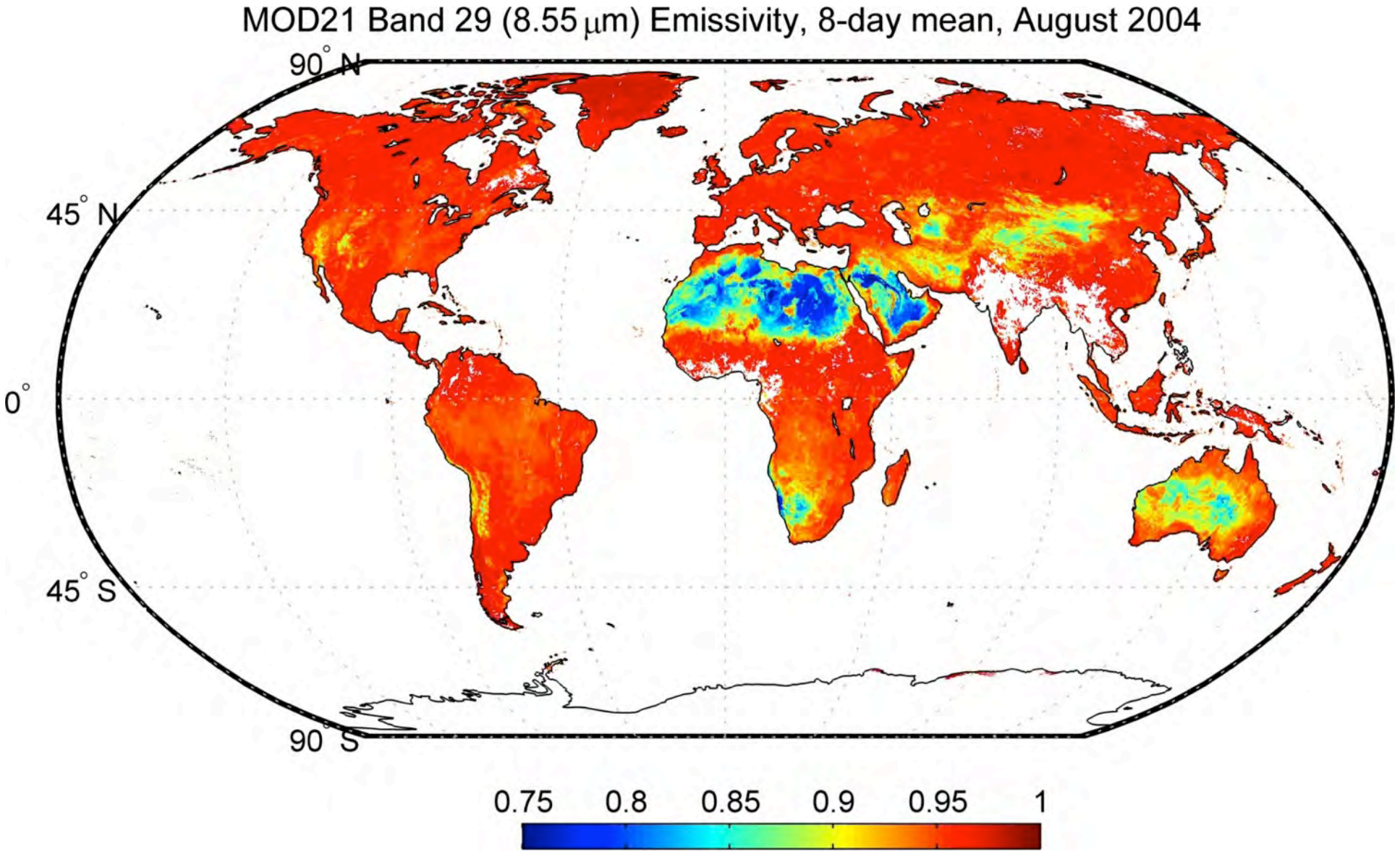

Generated using prototype MOD21 algorithm at MODAPS

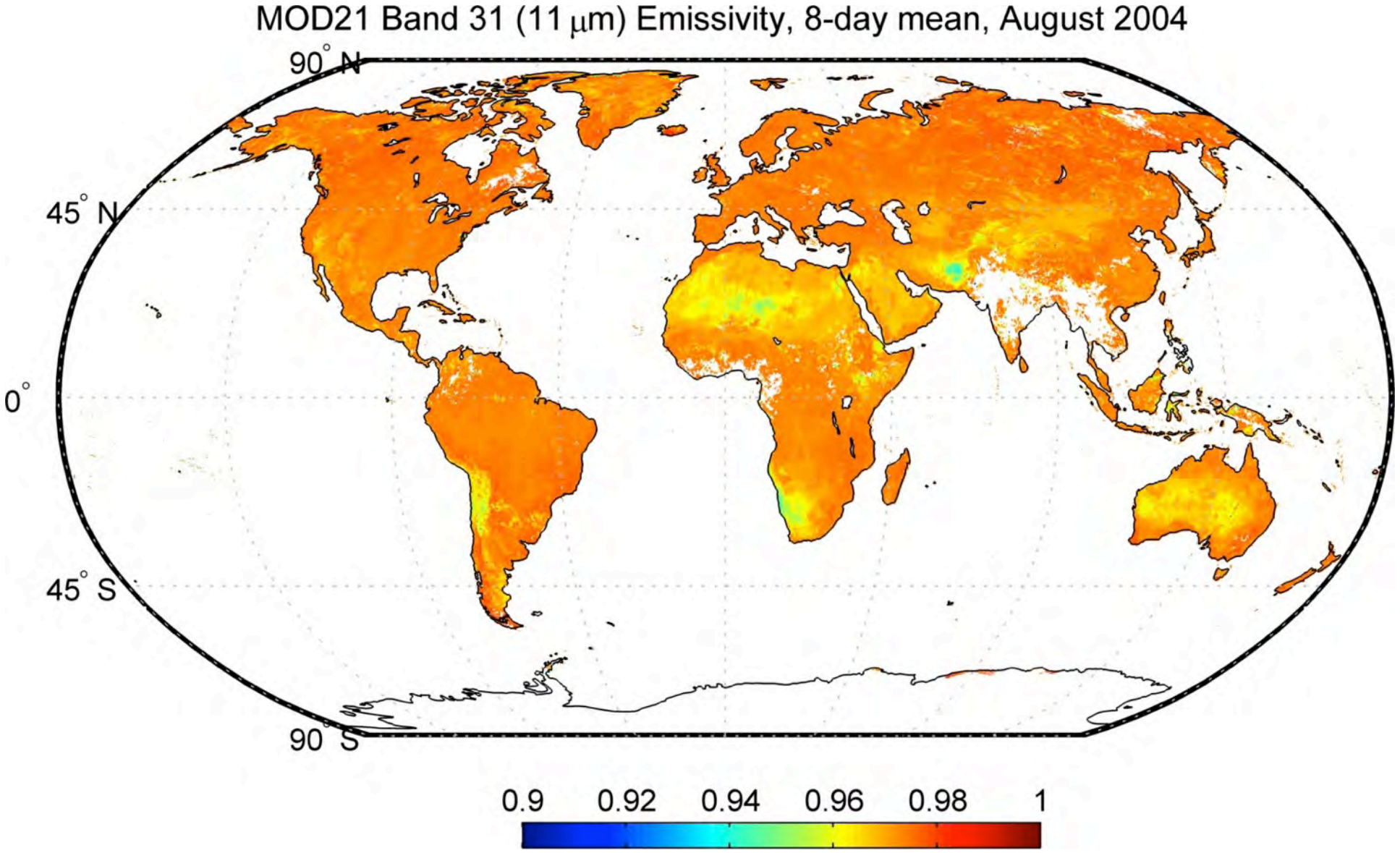

Generated using prototype MOD21 algorithm at MODAPS

Monitoring snow melt on Greenland using MOD21 emissivity and LST

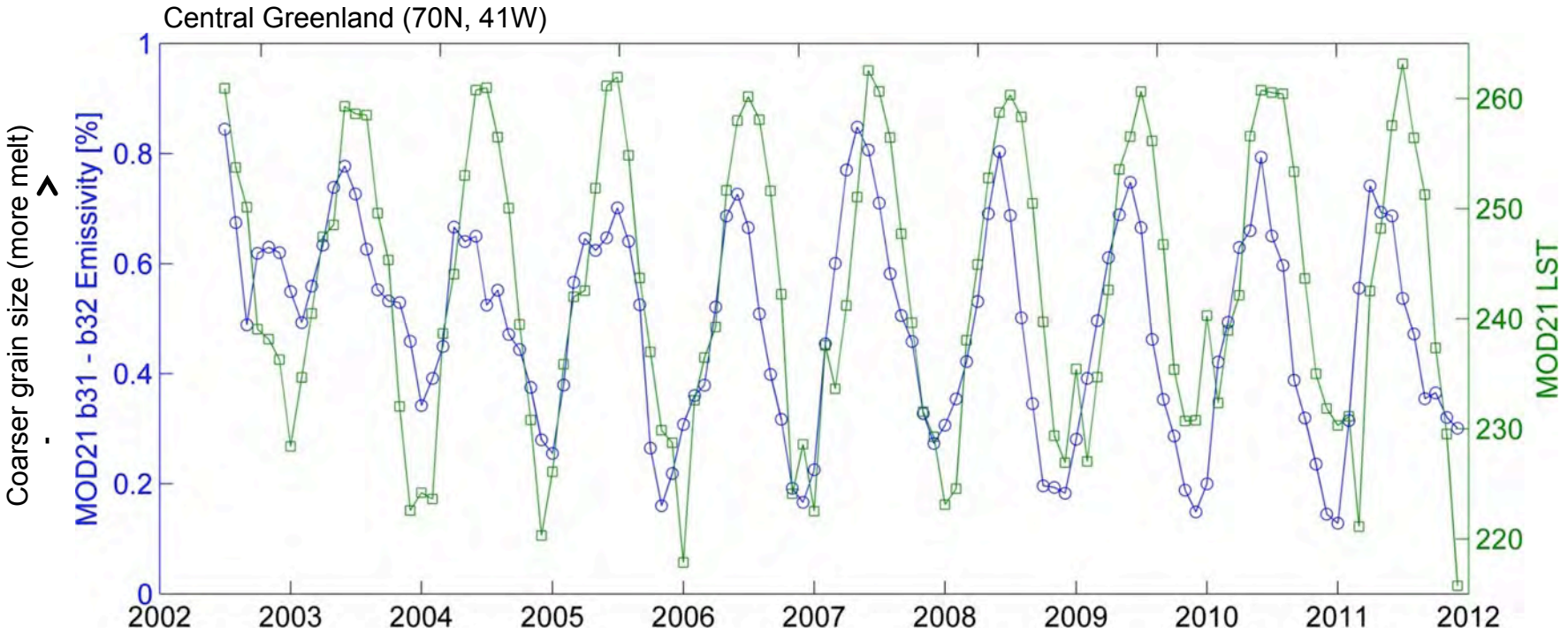

- Band 32 decreases with increasing snow grain size, while Band 31 is invariant
- Emissivity is an intrinsic property of the surface and will give more direct measure of snow/melt cycle on glaciers
- Day and night emissivity retrievals increases yield during difficult periods (e.g. during winter cloudy conditions)

Comparison with MCD43 Albedo Product

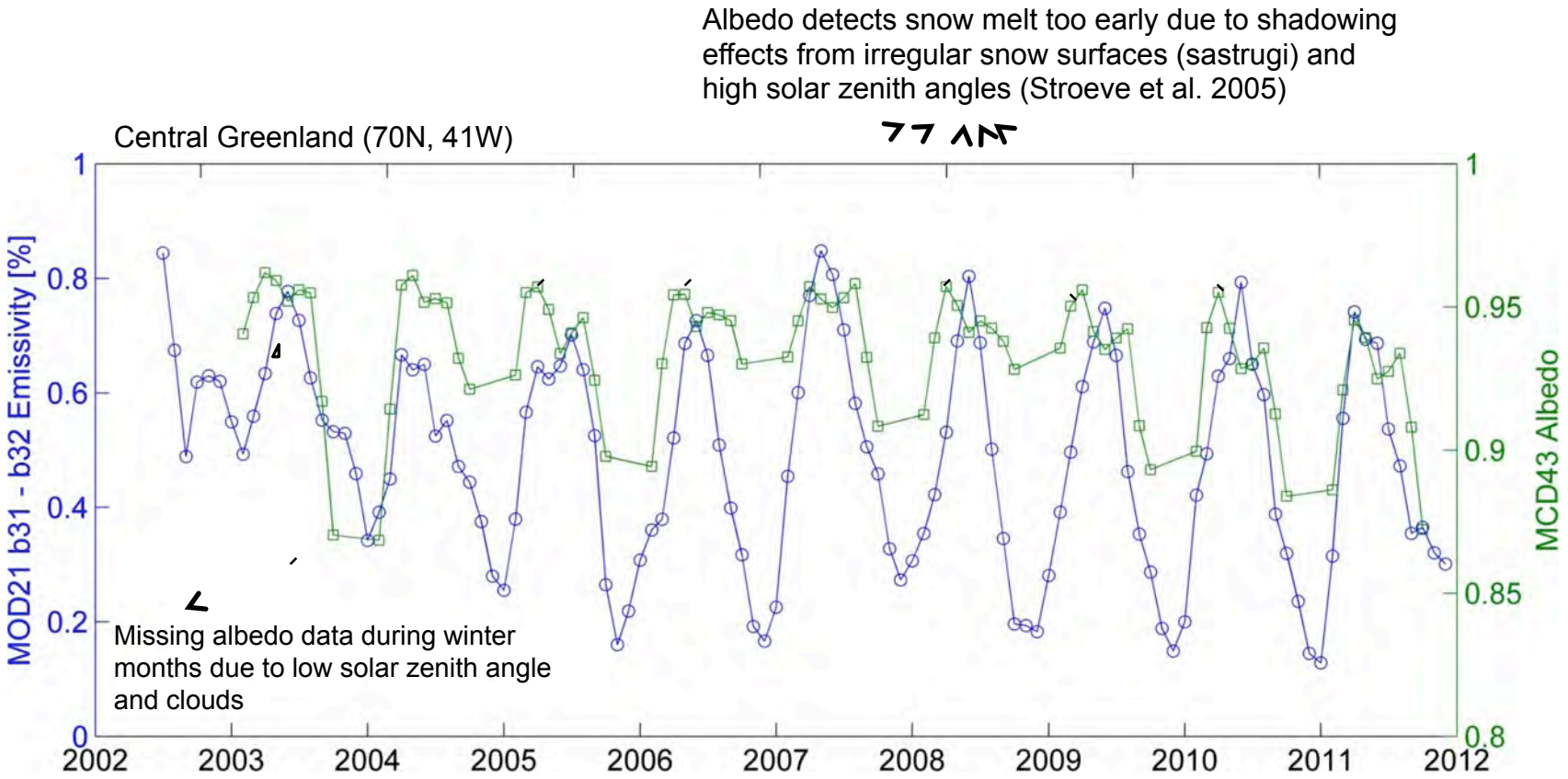

- Emissivity has higher sensitivity to snow melt intensity than albedo
- Emissivity is retrieved both day and night resulting in higher data yield under more difficult conditions during wintertime
- Albedo often detects snow melt too early due to shadowing from weathered snow features such as sastrugi

Monitoring land degradation (desertification) in dryland regions using MOD21 band 29 emissivity

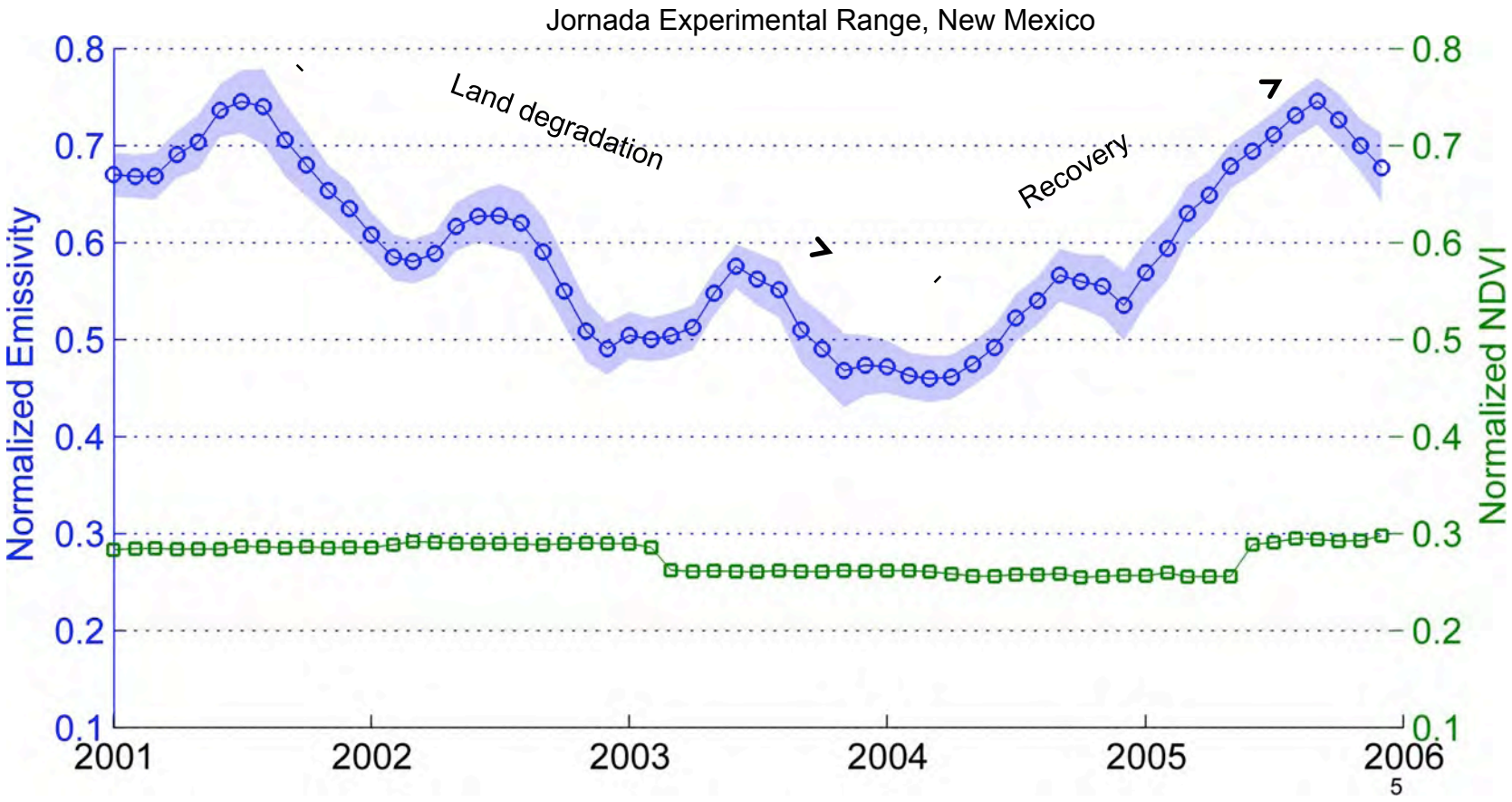

- Emissivity and NDVI normalized to their maximum and minimum ranges
- Band 29 emissivity sensitive to background soil and dry/green vegetation
- NDVI unable to make distinction between background soil and dry vegetation
- Emissivity able to better capture seasonal trends and interannual trends than NDVI

MOD21 and MOD11 LST Comparison

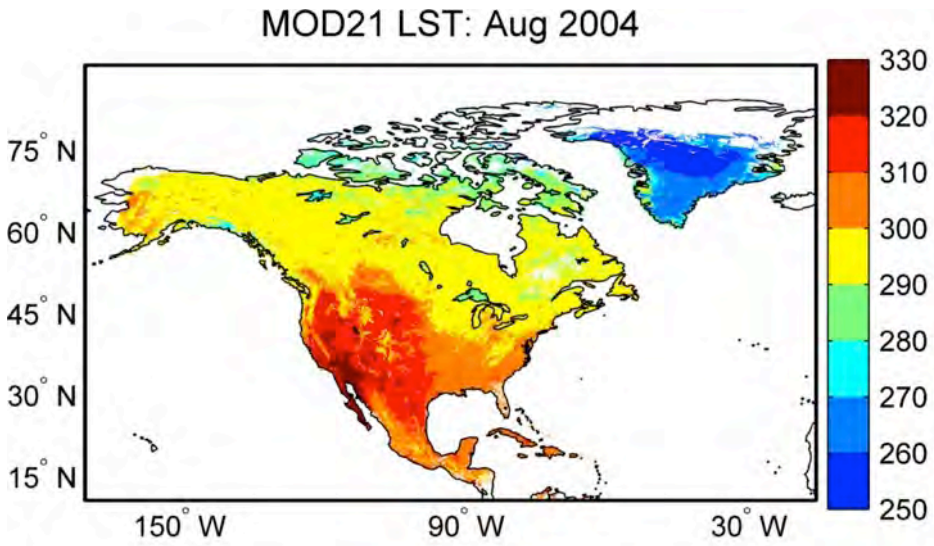

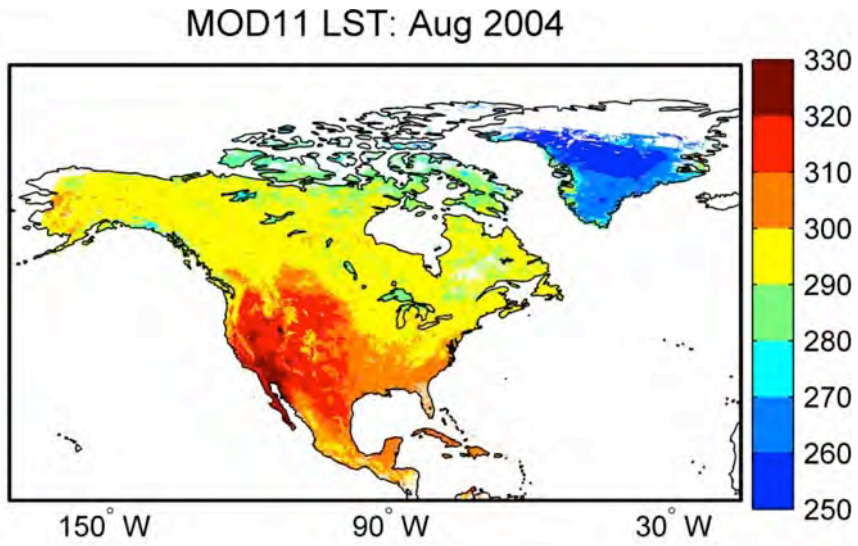

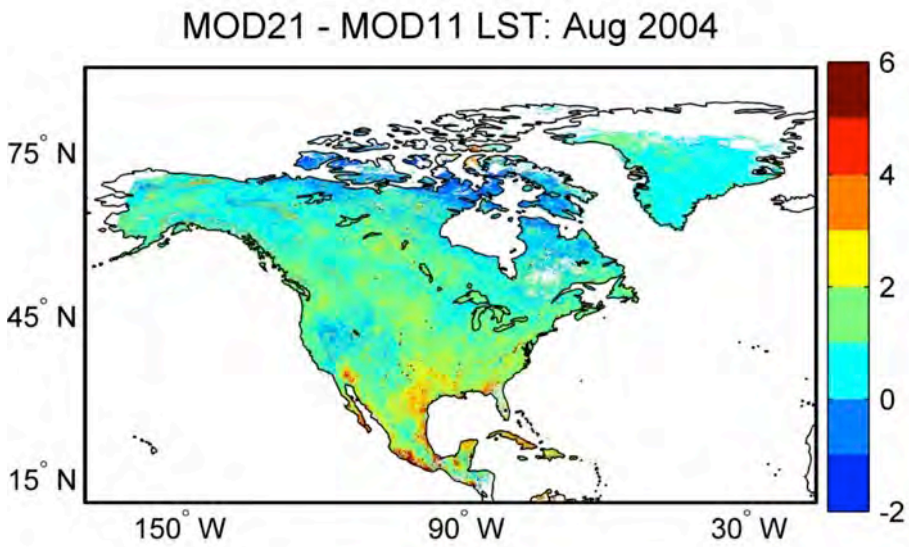

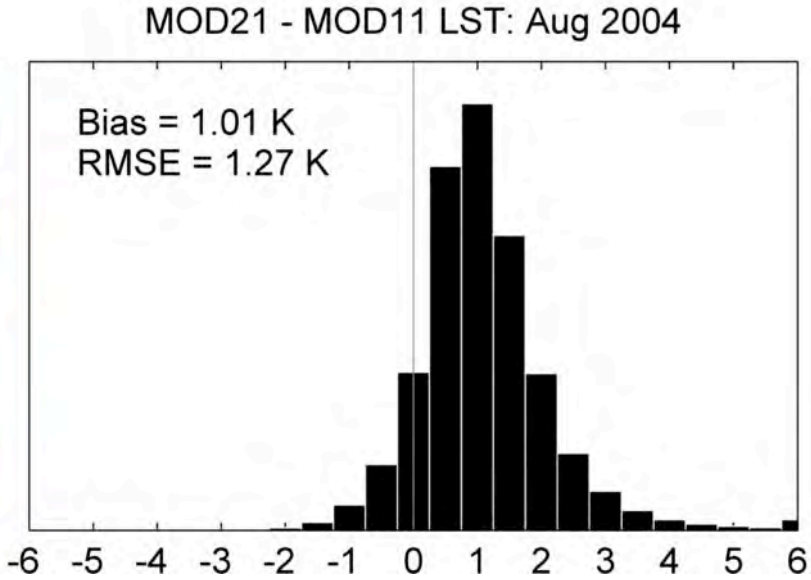

Large LST differences over bare regions and regions of high humidity – will these be smaller in Collection 6 ?

Emissivity Validation: Great Sands, Colorado

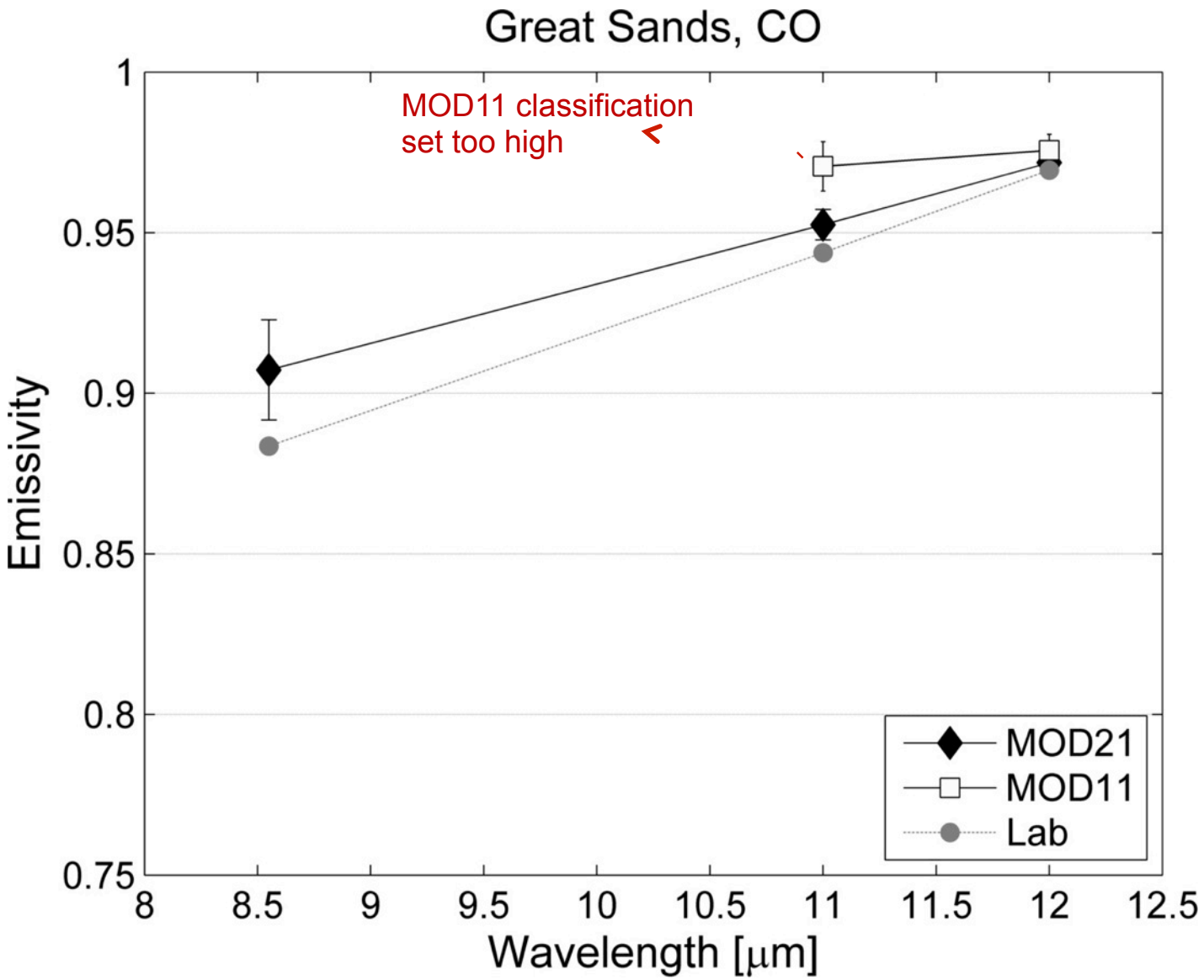

LST&E Validation Sites

Site name	Site type	Lat	Lon	Elevation (km)	Emissivity source	IGBP cover type (MOD12)	IGBP fraction (%)	Data availability
Bondville, IL	SURFRAD	40.05 N	88.37 W	0.213	ASTER (NAALSED)	Cropland	7.13	1994-present
Boulder, CO	SURFRAD	40.12 N	105.24 W	1.689	ASTER (NAALSED)	Grassland	5.87	1995-present
Fort Peck, MT	SURFRAD	48.31 N	105.10 W	0.634	ASTER (NAALSED)	Grassland	5.87	1994-present
Goodwin Creek, MS	SURFRAD	34.25 N	89.87 W	0.098	ASTER (NAALSED)	Cropland/Natural Vegetation	8.04	1994-present
Penn State, PA	SURFRAD	40.72 N	77.93 W	0.376	ASTER (NAALSED)	Cropland/Natural Vegetation	8.04	1998-present
Desert Rock, NV	SURFRAD	36.63 N	116.02 W	1	ASTER (NAALSED)	Shrublands	17.7	1998-present
Sioux Falls, SD	SURFRAD	43.73 N	96.62 W	0.473	ASTER (NAALSED)	Cropland	7.13	2003-present
Algodones, CA	PI Sand dune	32.95 N	115.07 W	0.094	In situ/Lab	Bare	9.11	n/a
Coral Pink, UT	PI Sand dune	37.04 N	112.72 W	1.78	In situ/Lab	Bare	9.11	n/a
Great Sands, CO	PI Sand dune	37.77 N	105.54 W	2.56	In situ/Lab	Bare	9.11	n/a
Kelso, CA	PI Sand dune	34.91 N	115.73 W	0.8	In situ/Lab	Bare	9.11	n/a
Killpecker, WY	PI Sand dune	41.98 N	109.1 W	2	In situ/Lab	Bare	9.11	n/a
Little Sahara, UT	PI Sand dune	39.7 N	112.39 W	1.56	In situ/Lab	Bare	9.11	n/a
Stovepipe Wells, CA	PI Sand dune	36.62 N	117.11 W	0	In situ/Lab	Bare	9.11	n/a
White Sands, NM	PI Sand dune	32.89 N	106.33 W	1.216	In situ/Lab	Bare	9.11	n/a
Namib desert, Namibia	PI Sand dune	24.45 S	15.35 E	0.828	In situ/Lab	Bare	9.11	n/a
Kalahari desert, Botswana	PI Sand dune	27.325 S	21.226 E	0.917	In situ/Lab	Shrublands	17.7	n/a
Redwood, CA	Graybody	41.4 N	123.7 W	0.796	ASTER speclib	Evergreen Needleleaf forest	4.12	n/a
Texas Grassland, TX	Graybody	36.29 N	102.57 W	1.28	In situ (Wan)	Grassland	5.87	n/a
Greenland	Graybody	70 N	41 W	0	ASTER speclib	Snow and Ice	~34	n/a
Tahoe, CA	EOS Cal/Val	39.153 N	120 W	1.9	ASTER speclib	Water	tbd	2000-present
Salton Sea, CA	EOS Cal/Val	33.248 N	115.725 W	0	ASTER speclib	Water	tbd	2008-present
Gobabeb, Namibia	LSA-SAF	23.55 S	15.05 E	0.408	In situ/Box Method	Bare	9.11	2008-present
Dahra, Senegal	LSA-SAF	15.34 N	15.49 W	0.09	Lab endmember fraction	Grassland	5.87	2009-present
Evora, Portugal	LSA-SAF	38.9 N	8.00 W	0.016	Lab endmember fraction	Savannas	4.23	2008-present
SURFRAD = NOAA Surface Radiation Budget Network (http://www.esrl.noaa.gov/gmd/grad/surfrad/index.html)								
PI Sand dune = Pseudo-invariant sand dune sites (JPL, http://emissivity.jpl.nasa.gov/validation)								
Graybody = graybody sites used for R-based validation at JPL								
In situ/Lab = Sand samples collected in the field and measured using a Nicolet spectrometer at JPL during 2008								
In situ (Wan) = Surface emissivity measured with a sun-shadow method in Dallam County, Texas in April 2005 by Zhengming Wan								

LST Validation: Great Sands, Colorado

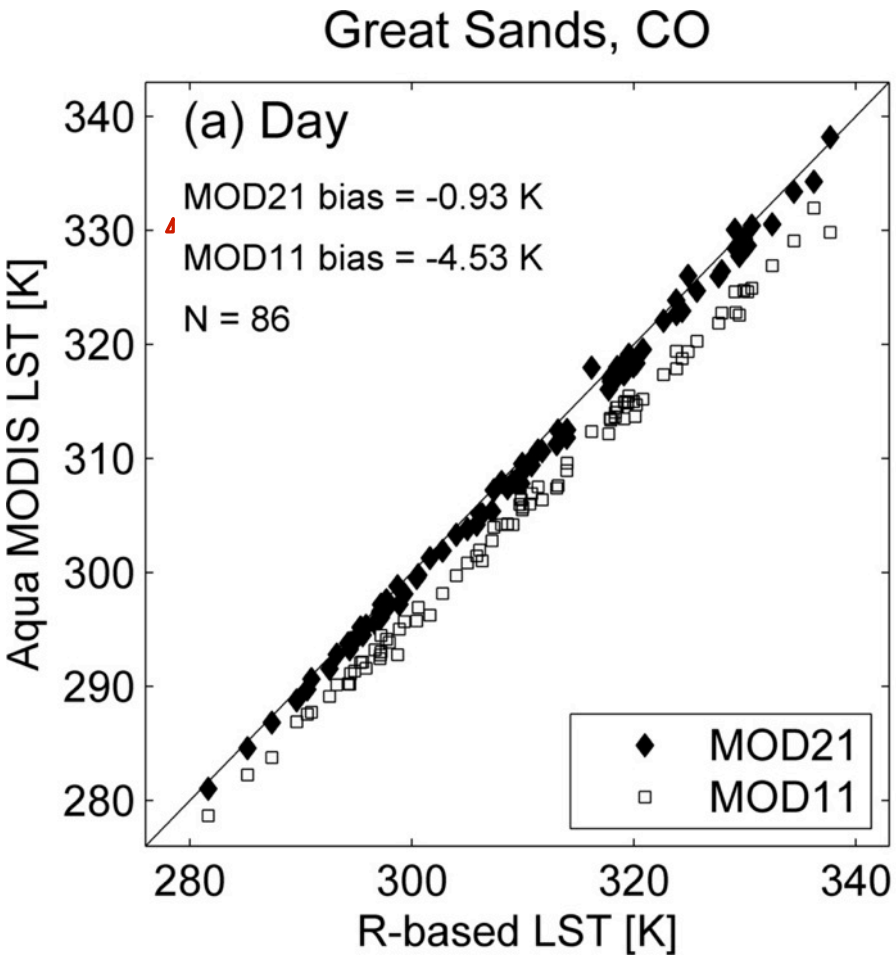

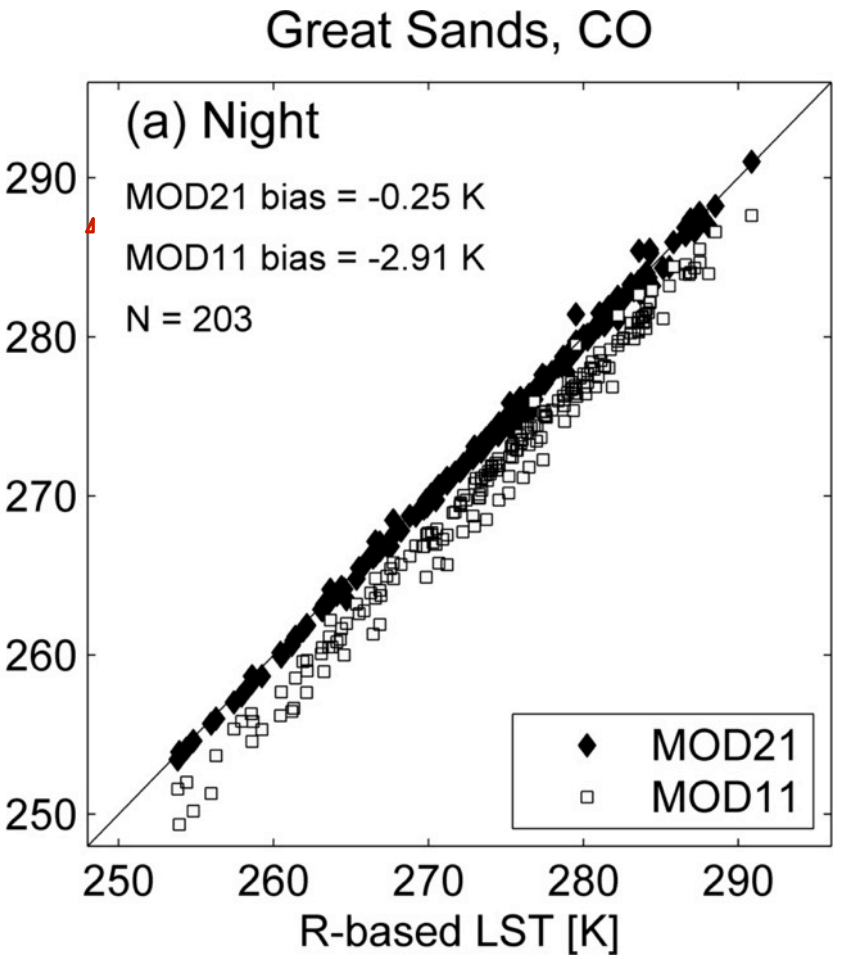

** Radiance-based LST validation using lab-measured sand samples collected at dune site

LST Validation: Greenland ice sheet

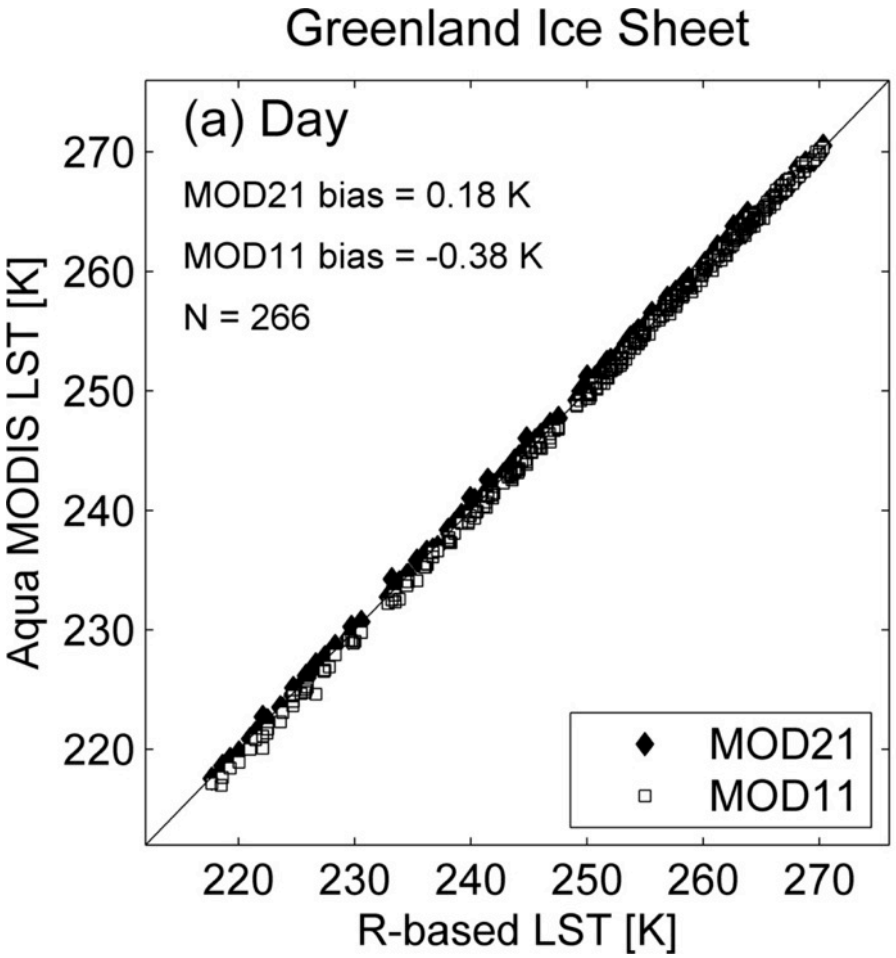

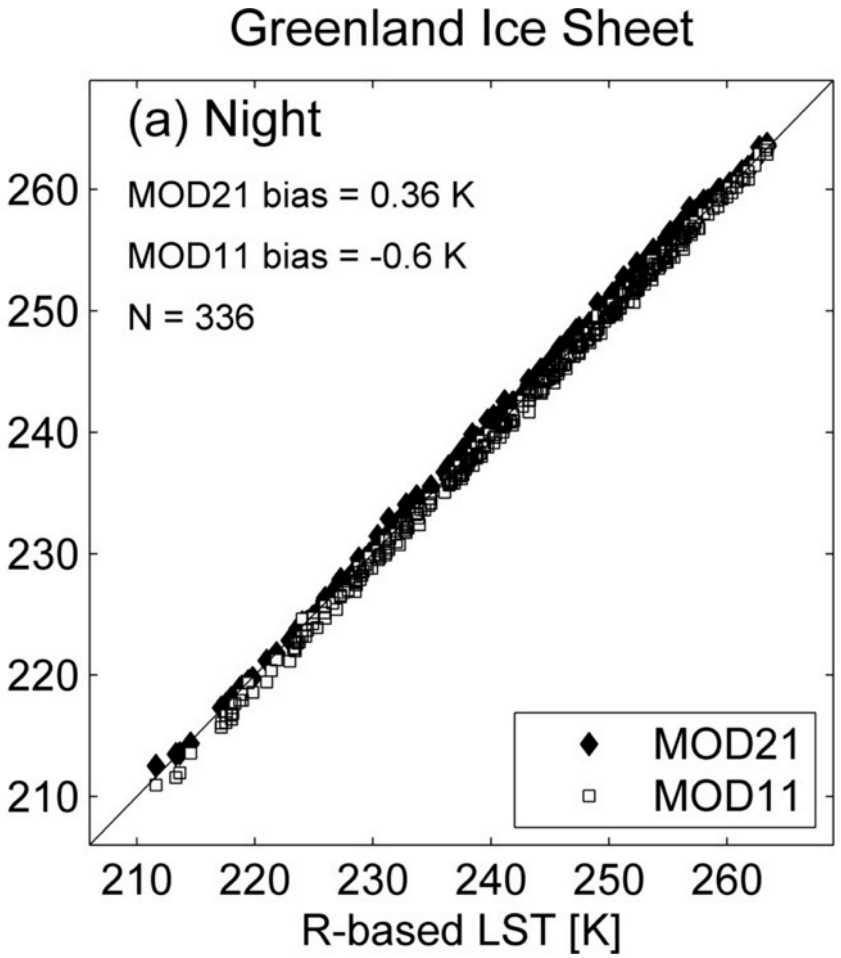

Similar accuracy over Greenland (<1 K)

LST Validation summary: Graybody surfaces (forest, snow/ice, grassland)

		Aqua Day		Aqua Night	
		MOD11	MOD21	MOD11	MOD21
Redwood Forest, CA 41.4 N, 123.7 W	Bias [K]	0.32	-0.34	0.19	-0.61
	RMSE [K]	0.56	0.61	0.60	0.96
Greenland 70 N, 41 W	Bias [K]	0.61	-0.33	0.34	-0.18
	RMSE [K]	0.73	0.50	0.56	0.35
Texas Grassland 36.29 N, 102.57 W	Bias [K]	0.59	0.24	0.66	0.59
	RMSE [K]	0.85	0.54	1.02	0.98

MOD21 and MOD11 have similar accuracy over graybody surfaces (<1 K)

LST Validation summary: Bare surfaces (pseudo-invariant sand sites)

Sites	Obs	MOD11	MOD21	MOD11	MOD21
		Bias (K)		RMSE (K)	
Algodones, CA	956	-2.89	-0.05	3.04	1.07
Great Sands, CO	546	-4.53	-0.93	4.63	1.17
Kelso, CA	759	-4.55	-1.48	4.62	1.67
Killpecker, WY	463	-4.51	-1.19	4.58	1.42
Little Sahara, UT	670	-3.71	-0.60	3.79	0.89
White Sands, NM	742	-0.73	-0.29	1.07	0.95

MOD11 cold bias of up to ~5 K over bare sites
(due to overestimated classification emissivity)

When looking for trends we need to worry about long-term calibration!

Delta Brightness Temperature in TIR Channels for MODIS Terra at Lake Tahoe and Salton Sea CY2000-2013 vz0-7 v5.x

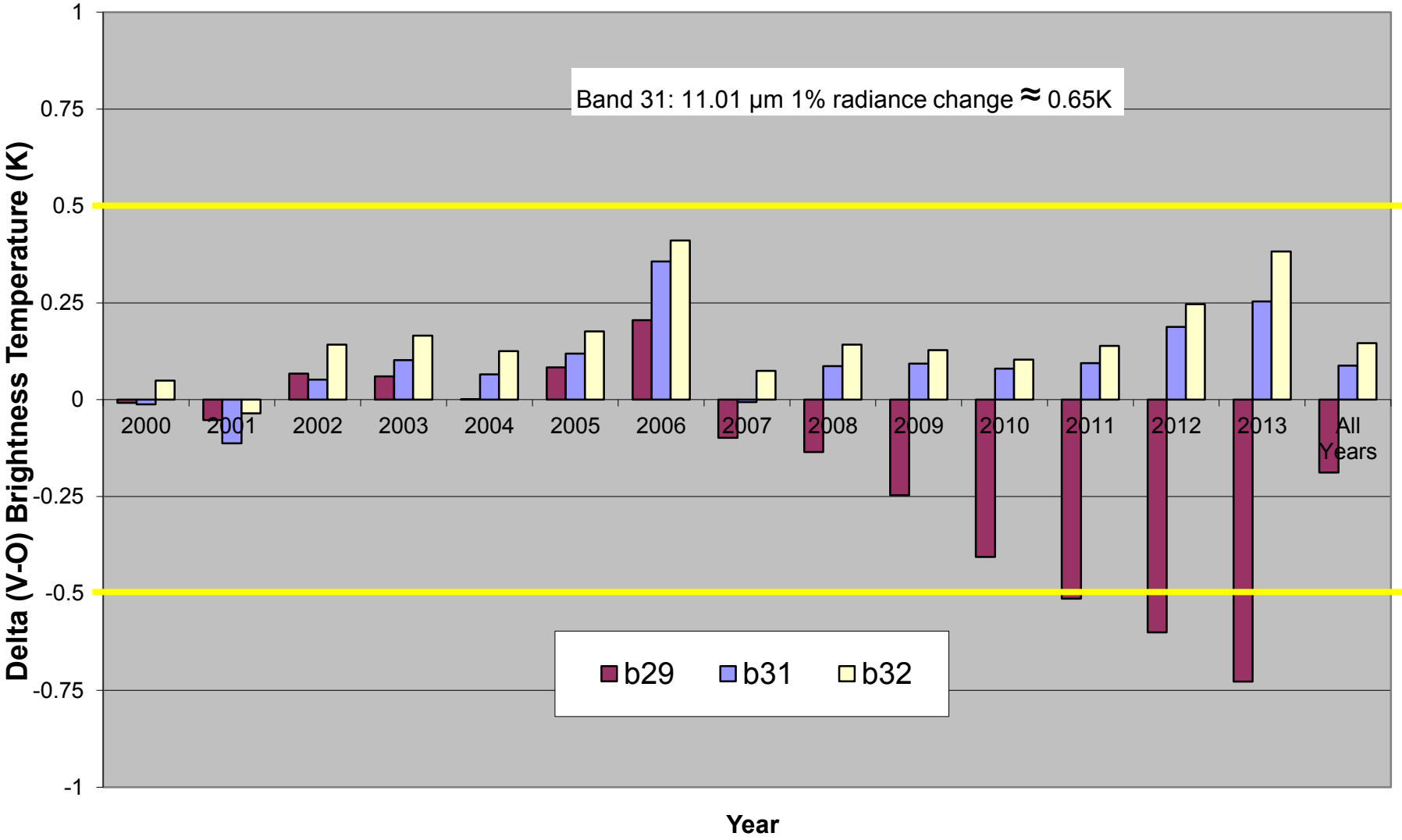

Excellent calibration until 2009. Since 2009 channel 29 calibration started to degrade

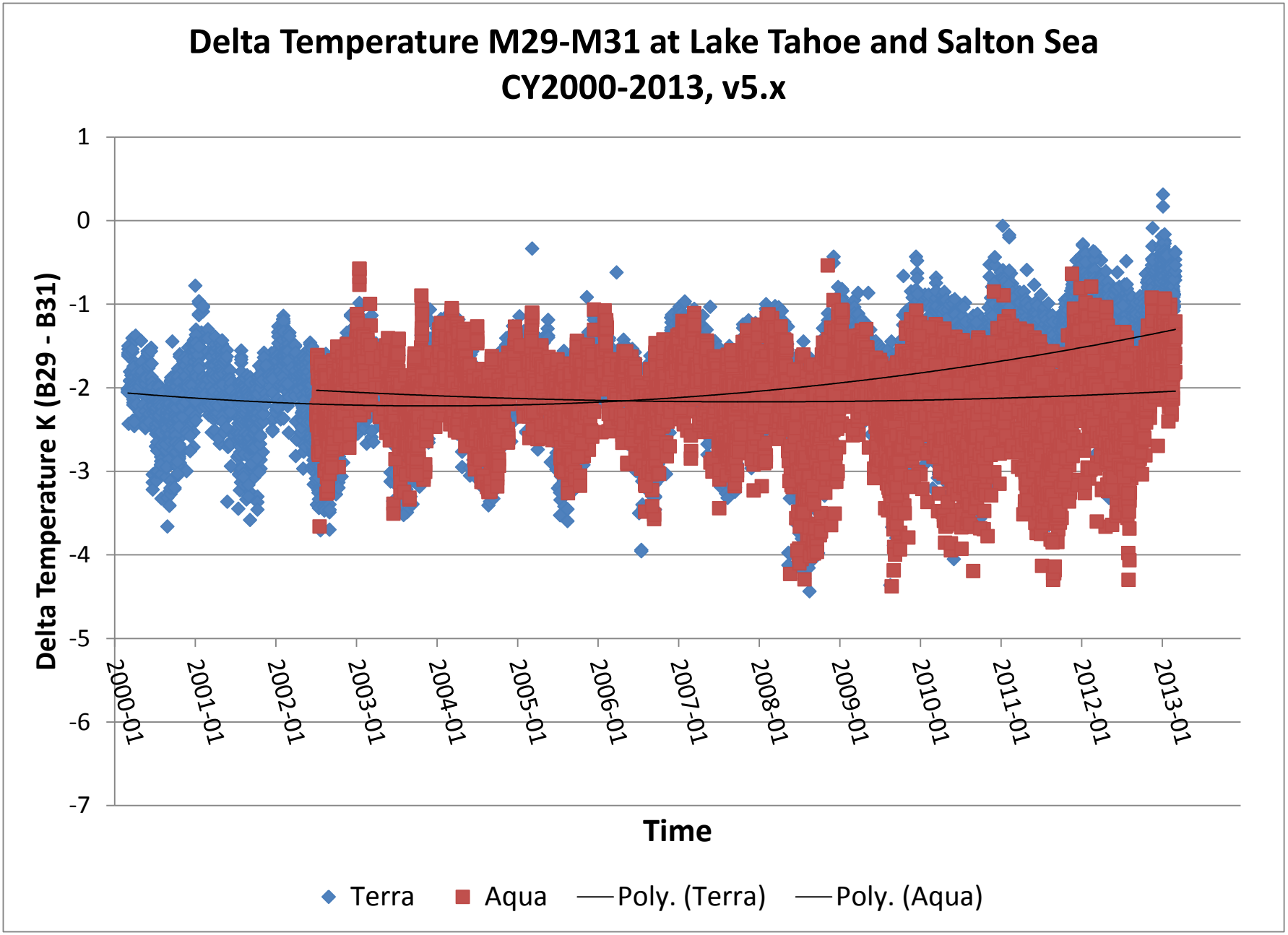

Similar analysis to previous slides but notice how range of Aqua data has increa

MOD21 LST&E Uncertainty Analysis

- LST&E Uncertainty Simulator (LSTE-US) developed at JPL
  - Global set of radiosonde profiles (382 from 1-6 cm total water vapor)
  - Broad range of surface characterization (>100 spectra from ASTER spectral library)
  - At-sensor radiances simulated for any given sensor's spectral response

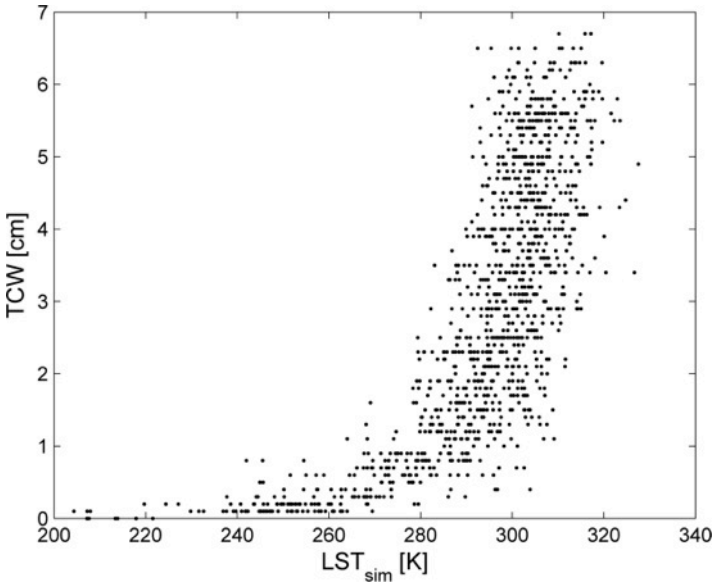

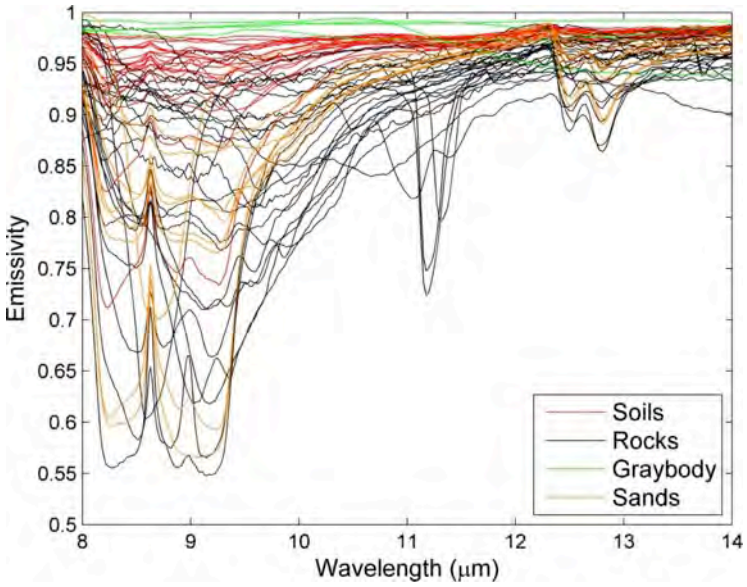

- Error contributions modeled:
  - Model or Algorithmic error
  - Atmospheric compensation error
  - Measurement noise error (NEDT)
  - Cloud contamination

MOD21 Uncertainty Parameterization

$$\delta LST_{MODIS} = a_o + a_1 TCW + a_2 \mathrm{SVA} + a_3 TCW \cdot SVA + a_4 TCW^2 + a_5 SVA^2 \qquad (10)$$

$\boldsymbol{a_i}$ = regression coefficients dependent on surface type (gray, bare, transition)
$\boldsymbol{SVA}$ = sensor view angle
$\boldsymbol{TCW}$ = total column water estimate (cm), e.g. from MOD07, NCEP

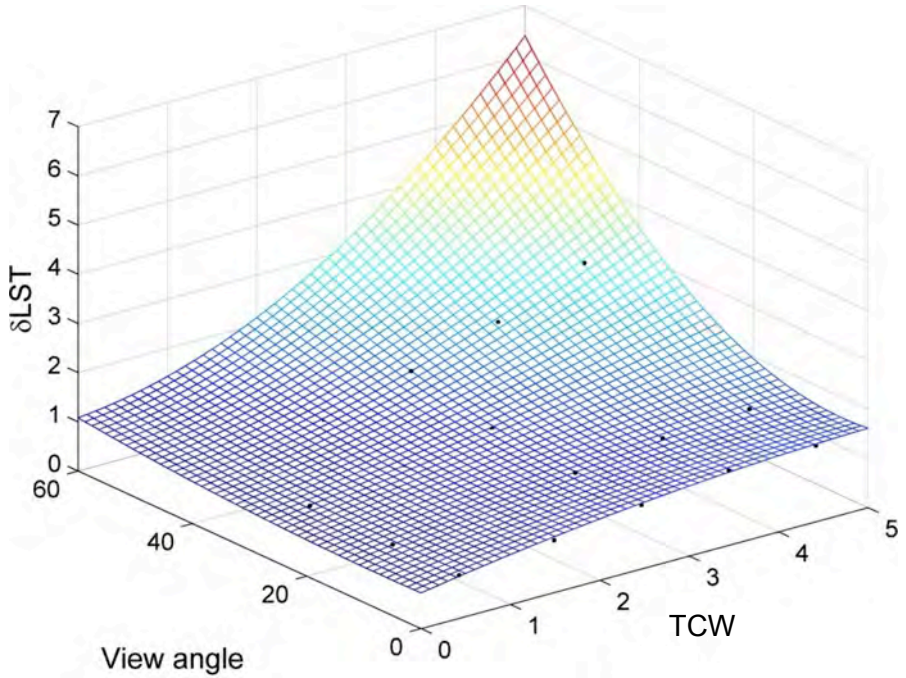

MOD21 LST&E Retrievals with Uncertainty

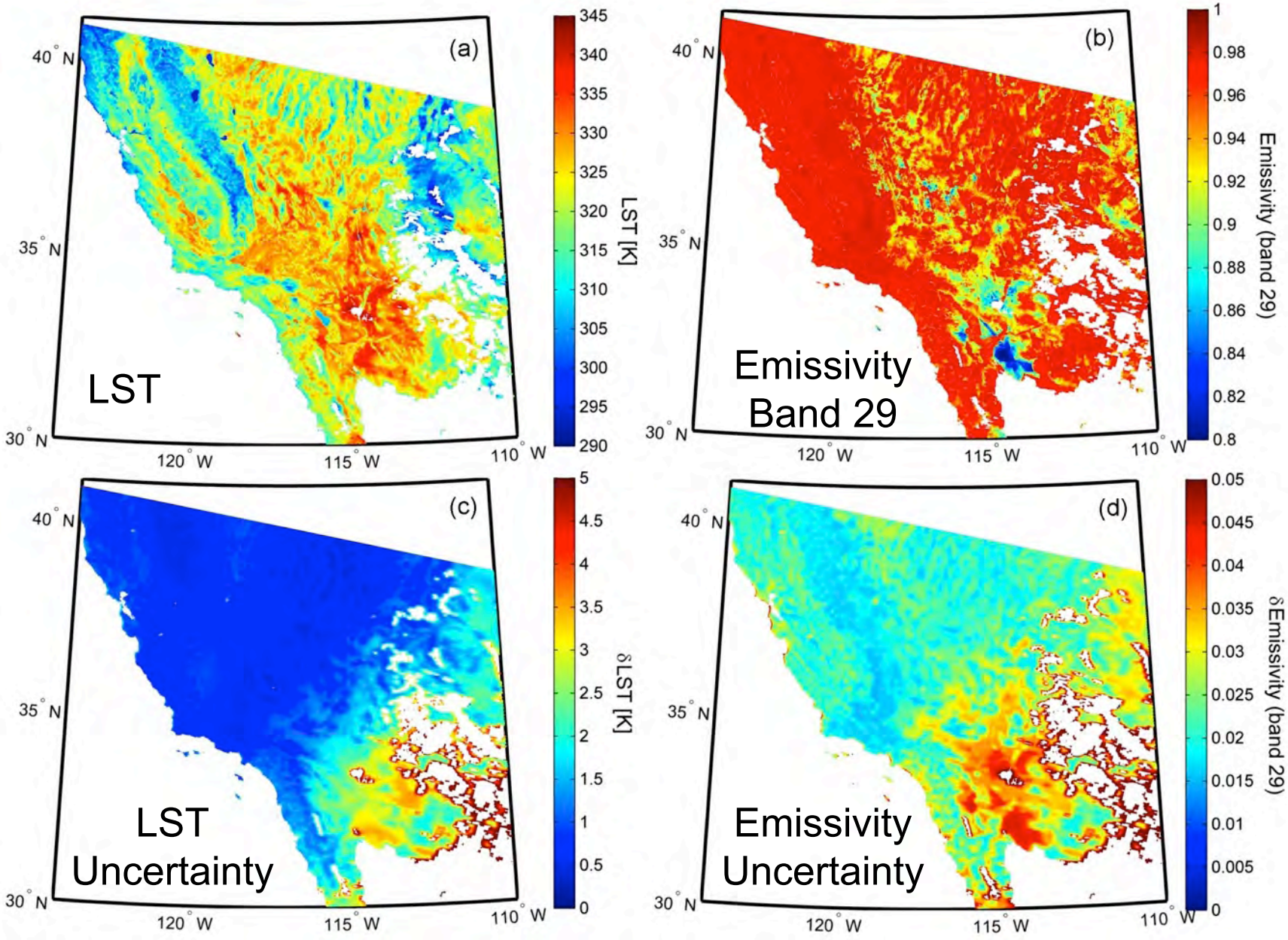

Future Work

- Continue to evaluate improvements in C6 to current MODIS algorithms
- Continue with development and optimization of MOD21 prototype algorithm at MODAPS (Ginny Kalb)
- Complete global 8-day test for summer and winter data
- Expand validation to use global set of sites
- Speed up grid-to-granulation process
- Improve water vapor scaling (WVS) method interpolation over bare surfaces using Kriging approach
- Incorporate option to use AIRS v6 profiles instead of MYD07 to improve accuracy of Aqua retrievals
- Release MOD21 with Collection 6

The End

National Aeronautics and Space Administration

Jet Propulsion Laboratory
California Institute of Technology
Pasadena, California

www.nasa.gov

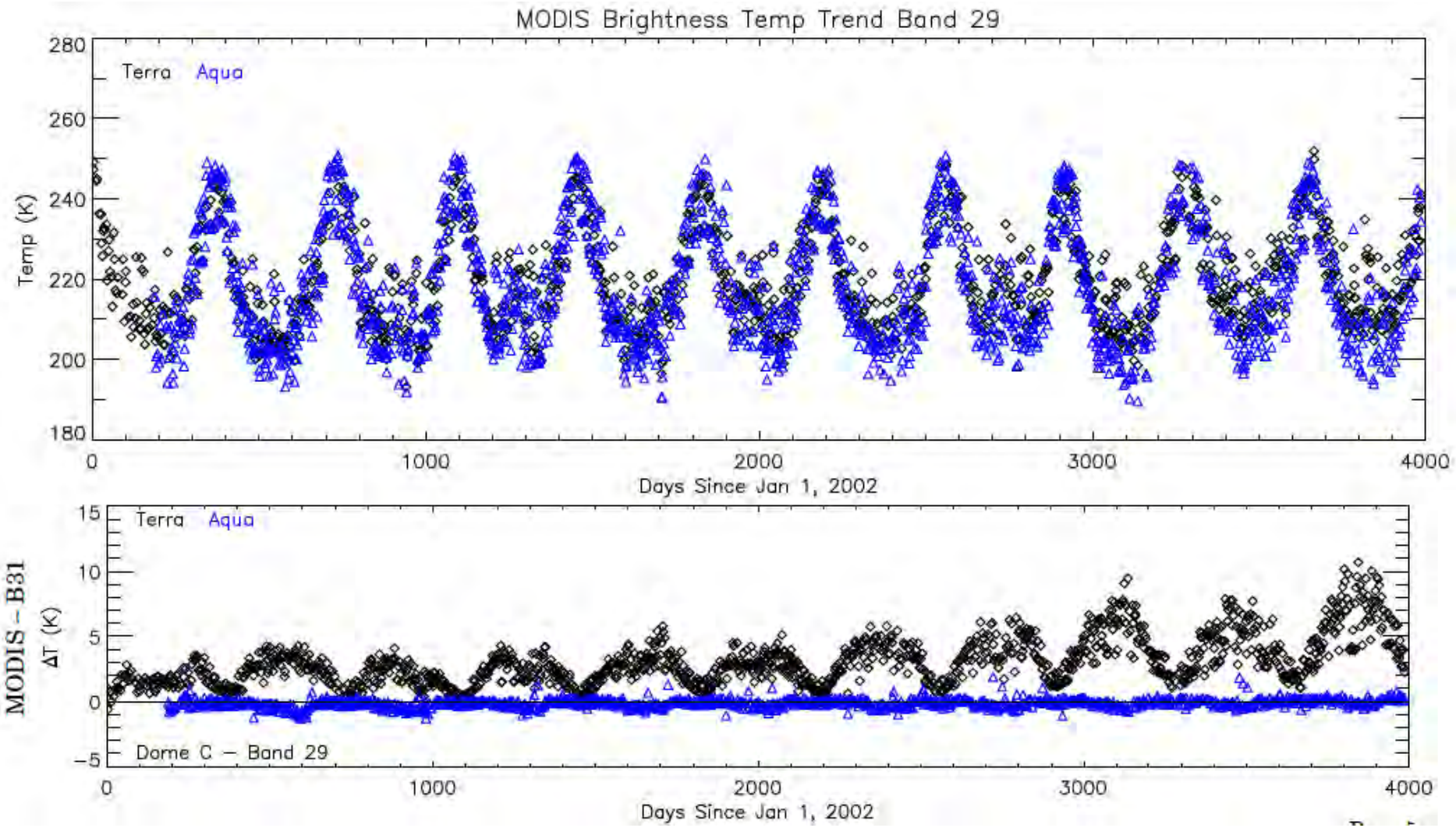

Analysis repeated by Brian Wenny and observed similar problem using Dome C. Problem is less severe in Collection 6 due to change in how a0 coefficient implemented in calibration equation

Trends (deseasonlized)

Trends calculated using the Breaks For Additive Season and Trend (BFAST) algorithm

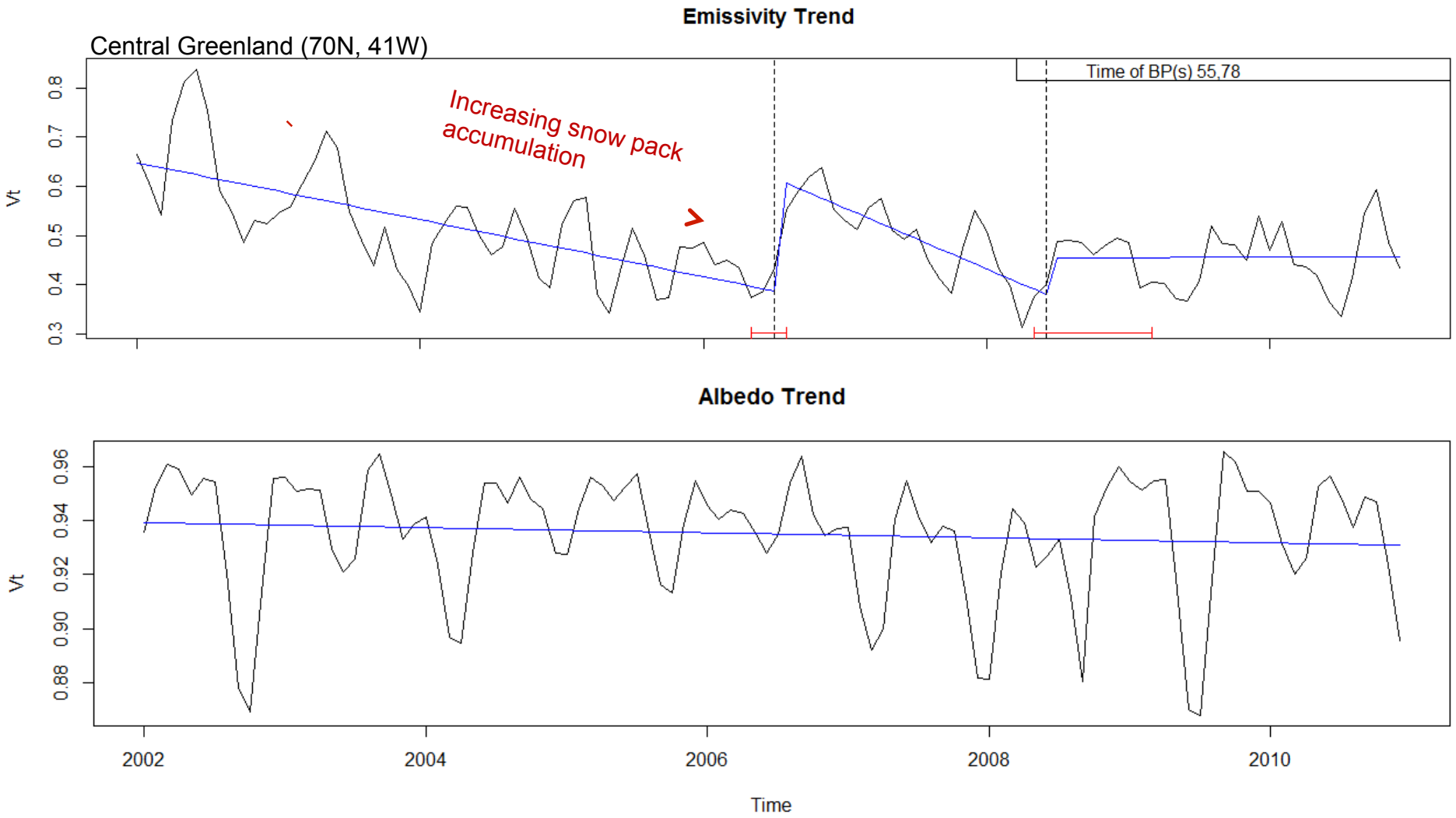

- Emissivity is more sensitive to snow variations than albedo
- Decreasing emissivity trends indicate an increase in snowpack and is consistent with observations of increased precipitation over Greenland due to a warmer climate

Split Window: Classification versus physical emissivity

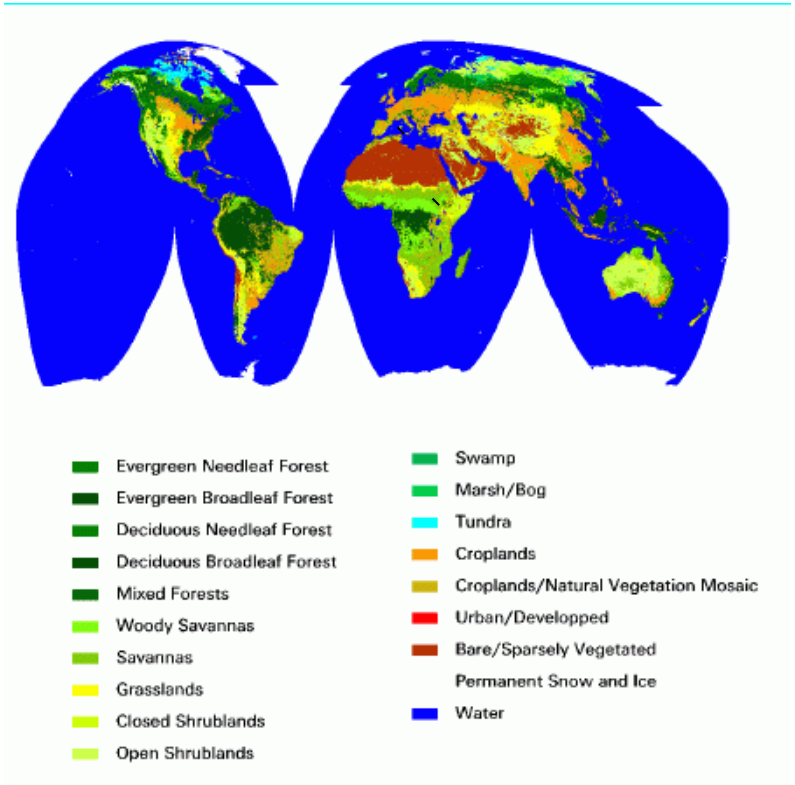

MOD11 band 31

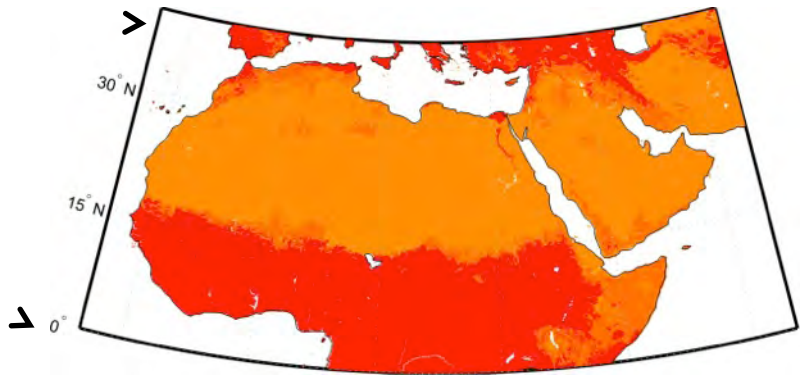

MOD21 band 31

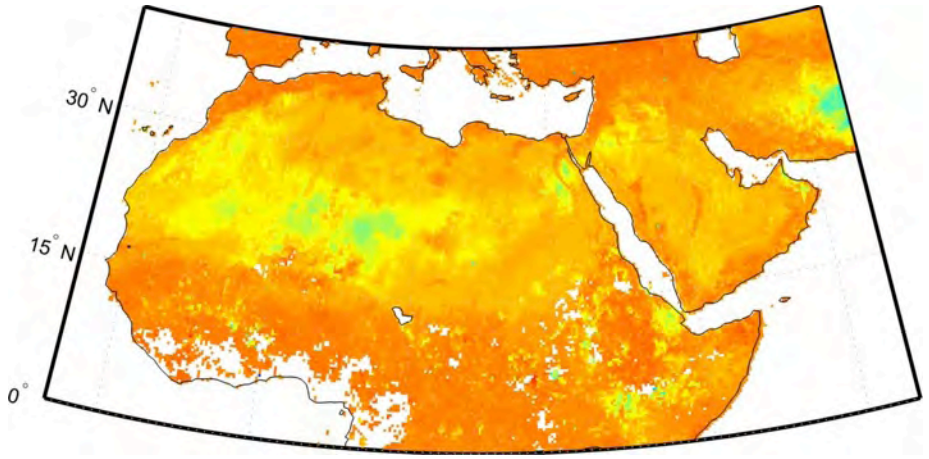

MOD11 classified as bare and assigned single emissivity but a wide range in emissivity is seen with MOD21